



ADT fast losses MD

Agnieszka Priebe, Tobias Baer, Bernd Dehning, Stefano Redaelli,
Belen Maria Salvachua Ferrando, Mariusz Sapinski,
Matteo Solfaroli Camillocci, Daniel Valuch, CERN, Geneva, Switzerland

Keywords: fast beam losses, the ADT, beam excitation, UFOs, collimators

Summary

The fast beam losses in the order of 1 ms are expected to be a potential major luminosity limitation for higher beam energies after the LHC long shutdown (LS1). Therefore a Quench Test is planned in the winter 2013 to estimate the quench limit in this timescale and revise the current models.

This experiment was devoted to determination the LHC Transverse Damper (ADT) as a system for fast losses induction. A non-standard operation of the ADT was used to develop the beam oscillation instead of suppressing them. The sign flip method had allowed us to create the fast losses within several LHC turns at 450 GeV during the previous test (26th March 2012). Thus, the ADT could be potentially used for the studies of the UFO ("Unidentified Falling Object") impact on the cold magnets. Verification of the system capability and investigations of the disturbed beam properties were the main objectives of this MD.

During the experiment, the pilot bunches of proton beam were excited independently in the horizontal and vertical planes to induce beam losses on the primary collimators (TCPs). An asymmetrical configuration of collimator jaws provided losses on only one side of an aperture. This created the conditions of a 3-corrector orbital bump Quench Test which is planned for winter 2013. The temporal loss distribution and the loss duration at 4 TeV were determined. The impact of the phase advance between the ADTs and TCPs was investigated at 450 GeV.

1 Introduction

The protection of the Large Hadron Collider superconducting magnets against a quenching and beam induced damage relies mainly on the Beam Loss Monitoring System (BLM). Ionization chambers detect secondary particles originating from the beam losses on the apertures. If the losses exceed a threshold value, the beam is extracted from the machine to the beam dump. The thresholds are set based on knowledge of quench levels (QLs) and they depend on the perturbation (loss) duration. The experience has shown that current knowledge of QL at millisecond timescale is not sufficient.

This experiment was devoted to the UFO ("Unidentified Falling Object") losses which are expected to be a potential major luminosity limitation for the higher beam energies[1]. Knowledge of the quench limit for the UFO-like losses is the final objective of our experiments (including the Quench Test foreseen in the winter 2013).

The LHC Transverse Damper (ADT) is a system which damps the beam oscillations under typical conditions of operation. There are three possible methods of ADT-induced beam excitation:

- 1) Coherent excitation (used for an injection/an abort gap cleaning)
- 2) White noise excitation (used for a controlled emittance blow-up and preparation of the loss maps)
- 3) Feedback sign flip (never used in a typical operation, a possible failure mode).

The loss induction capability of the ADT was explored during our studies since we used it for controlled beam loss investigations.

An experiment performed on 26th March 2012 (proton pilot bunches, 450 GeV beam energy, a nominal symmetrical configuration of the collimator jaws, [2], [3]) showed that the last mode provided the best loss properties in terms of a temporal loss distribution and a loss duration (Fig. 1). The main reason for this was the smallest amount of initial losses, i.e. the losses occurring before the peak value. An analysis of the Beam Position Monitor (BPM) signals showed that the beam amplitude rose the most regularly as well (Fig. 2). The feedback sign flip method allowed losses in the order of 6 LHC turns ($\sim 550 \mu\text{s}$) to be created at injection energy making it a good option for the UFO-like losses studies. Nevertheless, the higher the beam energy is, the more rigid the beam become. Therefore additional investigations were required to determine the ADT-induced loss duration at 4 TeV.

In the case of the sign flip technique, the higher the gain is, the faster the oscillation amplitude increases. This means that the probability that the beam hits the target in a single turn is higher. At a lower gain the situation is the opposite - the oscillations are built up slower so the beam is scraped over several turns.

The data collected on 22th June 2012 was associated with LHC fill 2756.

The ADT fast losses MD was a part of a preparation for the Quench Test at the nominal energy foreseen in the winter 2013 [4], [5].

2 Motivation

The main aims of the experiment were:

1. Creating the conditions of the fast ($\sim 1 \text{ ms}$) proton beam losses which are most similar to the Quench Test foreseen in the winter 2013 (Fig. 3 with a brief description)
2. Studying the ADT system as a tool for loss induction
3. Investigating the impact of the phase advance between the transverse dampers and the collimators on:
 - Excitation efficiency
 - Time structure
 - Loss efficiency

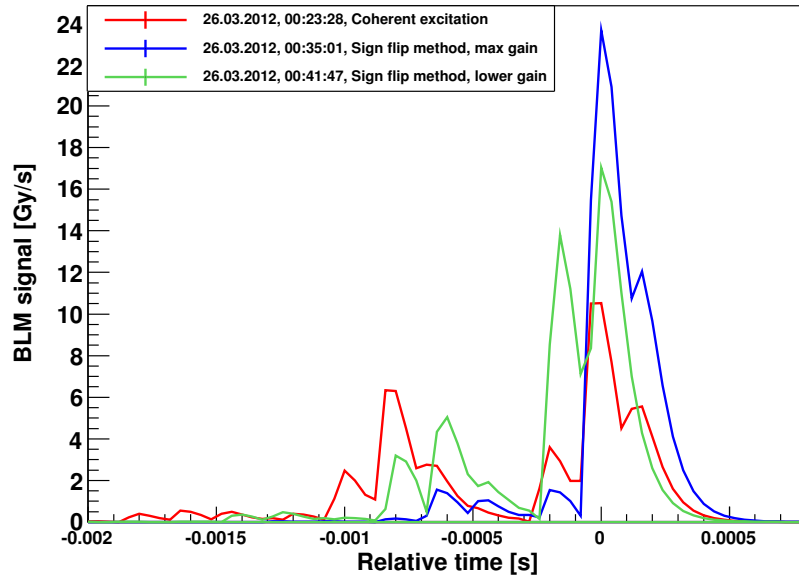


Figure 1: A comparison of the different modes of the ADT system (test of 26th March 2012). The temporal loss distributions show that the feedback sign flip method at maximum gain is the optimal candidate for the UFO timescale losses investigations.

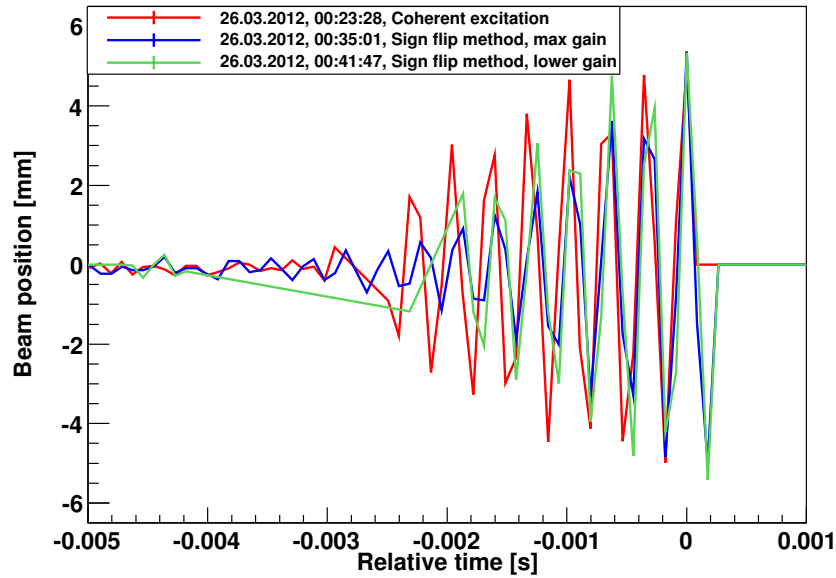


Figure 2: The beam transverse oscillations as a function of time. The ADT sign flip method with the maximum gain provides the most steady and close to linear increase of the beam amplitudes (test on 26th March 2012).

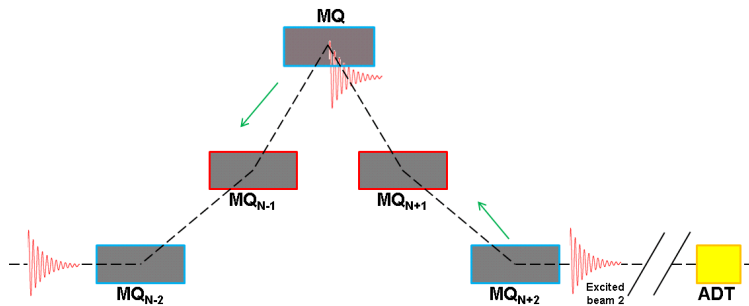


Figure 3: A combination of the 3-corrector orbital bump with the ADT beam excitation is one of the proposed methods for the fast and controlled loss induction. The beam is deflected by the MQ_{N+2} and aimed onto the MQ . A synchronization between the bump amplitude and the beam position will result in fast losses with the imposed loss duration.

3 Experimental conditions

The main idea of the MD was to excite the proton beam with the ADT and observe the induced losses on the primary collimators. An asymmetrical configuration of collimator jaws provided losses on one side of an aperture only. Since losses during the Quench Tests are induced in the direction outside of the coldmass centre¹, corresponding conditions were applied during this test. Therefore, an internal collimator jaw was aimed in the case of beam 1 and an external collimator jaw in the case of beam 2. The losses in the vertical plane were provided on an upper jaw. One-plane excitation was introduced.

The MD was performed on 22nd June 2012 and consisted of two parts devoted to different studies under slightly varied operation conditions.

3.1 Experiment at injection energy (450 GeV)

The determination of the impact of phase advance between the ADT and the collimator was the main objective for the first part of the experiment. Four cases (both beams and both excitation planes) were considered. Two configurations of the collimator settings were applied (Fig. 4 and Tab. 1) depending on the conditions of the LHC and the correlated machine protection. Beam 2 was considered safer because of the better splice quality in the magnet interconnections (Sector 6-7) where the additional losses could potentially occur[5]. Therefore the larger collimator apertures were accepted. The BLM monitor factors were decreased from 1.0 to 0.3 at the target locations (collimators) to comprise the safe operation of the accelerator on one hand (since the collimator jaw positions were changed) and the Post Mortem data acquisition on the other hand.

In the case of beam 1 all collimators were left at their nominal positions except for one which was moved 4σ towards the beam. In the case of beam 2, all collimator jaws were retracted to 11σ except one which was left at the nominal position of 5.7σ . Moreover, the TDIs were moved ± 10 mm and the TCLIs were retracted to the parking positions.

The ADT excitation was set in the appropriate plane (horizontal or vertical) at the maximum (100%) gain. The excitation sign was changed to the opposite one. This manoeuvre provided the beam excitation instead of beam damping. Under typical conditions of LHC

¹The outside of the coldmass corresponds to a part of the magnet which is the closest to the BLM monitor. This means that a particle shower travels through a half of the magnet only (it does not cross the aperture of the opposite beam).

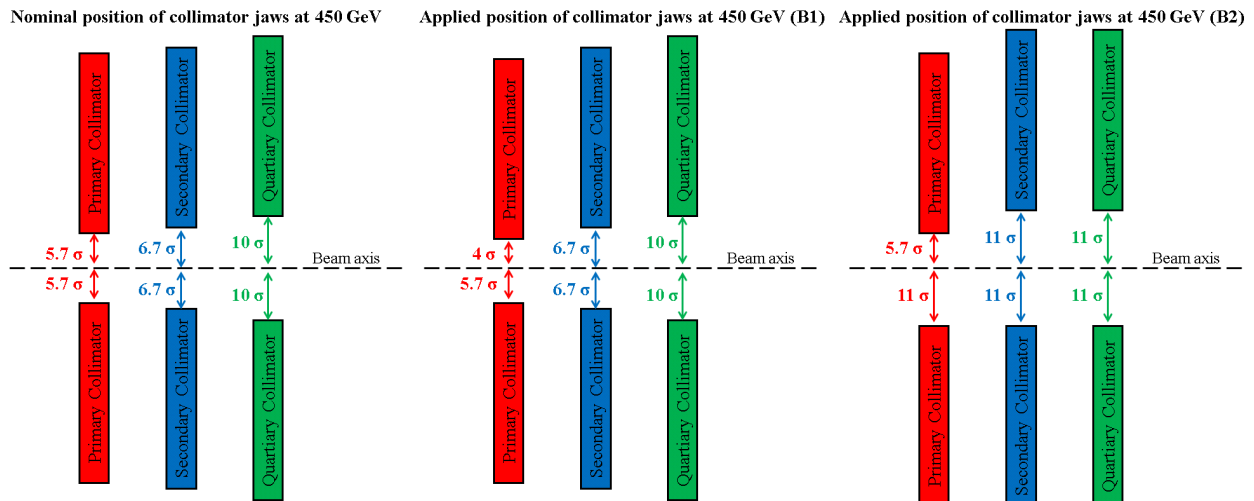


Figure 4: A scheme of the collimators configuration for 450 GeV beam. Left picture shows the nominal conditions, center and right - the positions applied during the test for beam 1 and beam 2, correspondingly (not to scale).

Table 1: Collimator settings at 450 GeV. All dimensions given in millimeters. σ_{nom} corresponds to the nominal σ , BB stands for the beam based center, J_L - left (upper) jaw, J_R - right (lower) jaw.

| Target half gap | | | | | Initial settings | | Beam 1 | Beam 2 |
|-----------------|-------|-------------|-----------|----------------|------------------|-------------|-----------|------------|
| | | | | | 5.7σ | 5.7σ | 4σ | 11σ |
| Beam | Plane | Collimator | BB centre | σ_{nom} | J_L | J_R | J_L | J_R |
| 1 | Hor | TCP.C6L7.B1 | -0.098 | 1.048 | 5.875 | -6.071 | 4.093 | -11.624 |
| 1 | Ver | TCP.D6L7.B1 | 0.235 | 0.756 | 4.543 | -4.073 | 3.258 | -8.078 |
| 2 | Hor | TCP.C6R7.B2 | 0.360 | 1.048 | 6.331 | -5.611 | 4.550 | -11.163 |
| 2 | Ver | TCP.D6R7.B2 | 0.730 | 0.756 | 5.038 | -3.578 | 3.753 | -7.583 |

Table 2: Wire Scanner measurements - the beam size. Each data set consists of two values: σ_{in} , taken when the wire goes through the beam, and σ_{out} - when the wire returns to its parking position. Usually, the average value σ_{avg} is used for analysis.

| Case | Time | Scan | σ_{in} [mm] | σ_{out} [mm] | σ_{avg} [mm] |
|------|----------|------|--------------------|---------------------|---------------------|
| B2H | 10:51:55 | Ver | 1.603 | 1.585 | 1.594 |
| B2V | 11:07:16 | Hor | 0.898 | 0.894 | 0.896 |
| | 11:06:33 | Ver | 1.699 | 1.715 | 1.707 |
| B1H | 11:30:06 | Hor | 1.027 | 1.001 | 1.014 |
| | 11:30:44 | Ver | 1.501 | 1.507 | 1.504 |
| B1V | 11:37:56 | Hor | 1.034 | 1.025 | 1.0295 |
| | 11:37:17 | Ver | 1.447 | 1.450 | 1.4485 |

Table 3: The LHC elements which were used during the MD. The ADTs were applied as the sources of a beam disturbance when the collimators played role of the targets.

| No. | Beam | Excitation plane | ADT | Collimator |
|-----|------|------------------|---------------|-------------|
| 1 | 2 | Horizontal | ADTKH.A5R4.B2 | TCP.C6R7.B2 |
| 2 | 2 | Vertical | ADTKV.A5L4.B2 | TCP.D6R7.B2 |
| 3 | 1 | Horizontal | ADTKH.A5L4.B1 | TCP.C6L7.B1 |
| 4 | 1 | Vertical | ADTKV.A5R4.B1 | TCP.D6L7.B1 |

Table 4: The locations of ADTs, TCPs and BLMs along the LHC ring (dcum).

| Element | Name | Dcum [m] |
|---------|------------------------------|------------|
| ADT | ADTKH.A5L4.B1 | 9971.9142 |
| | ADTKV.A5R4.B1 | 10023.0482 |
| | ADTKH.A5R4.B2 | 10022.2482 |
| | ADTKV.A5L4.B2 | 9971.1142 |
| TCP | TCP.C6L7.B1 | 19791.1844 |
| | TCP.D6L7.B1 | 19789.1844 |
| | TCP.C6R7.B2 | 20197.1404 |
| | TCP.D6R7.B2 | 20199.1404 |
| BLM | BLMEI.06L7.B1E10_TCP.C6L7.B1 | 19792.1840 |
| | BLMEI.06L7.B1E10_TCP.D6L7.B1 | 19790.1840 |
| | BLMEI.06R7.B2I10_TCP.C6R7.B2 | 20196.1400 |
| | BLMEI.06R7.B2I10_TCP.D6R7.B2 | 20198.1400 |

Table 5: The 450 GeV tests: the initial beam intensities and the timestamps of the beam dumps (Post Mortem data, local time)

| Case | Initial beam intensity [no of protons] | Time of the beam dump |
|------|--|-----------------------|
| B2H | 0.92e+10 | 10:57:32 |
| B2V | 1.13e+10 | 11:08:11 |
| B1H | 1.20e+10 | 11:31:39 |
| B1V | 1.40e+10 | 11:39:28 |

Table 6: 450 GeV tests, Logging Data Base: the beam intensities measured in the LHC ring and in the beam bump. The BCTFR corresponds to the Fast Beam Current Transformer in the ring, the BCTFD - in the beam dump.

| Case | Time | Monitor | Beam intensity [10^9 protons] |
|------|--------------|-----------------|----------------------------------|
| B2H | 10:57:32.117 | BCTFR.A6R4.B2 | 7.8 |
| | 10:57:32.816 | BCTFD.623139.B2 | 4.8 |
| B2V | 11:08:11.117 | BCTFR.A6R4.B2 | 9.2 |
| | 11:08:11.213 | BCTFD.623130.B2 | 7.7 |
| | 11:08:11.213 | BCTFD.623139.B2 | 6.7 |
| B1H | 11:31:39.057 | BCTFR.A6R4.B1 | 8.2 |
| | 11:31:39.054 | BCTFR.B6R4.B1 | 7.6 |
| | 11:31:39.398 | BCTFD.683130.B1 | 3.7 |
| B1V | 11:39:28.118 | BCTFR.A6R4.B1 | 10.6 |
| | 11:39:28.054 | BCTFR.B6R4.B1 | 9.8 |
| | 11:39:28.969 | BCTFD.683130.B1 | 9.0 |
| | 11:39:28.969 | BCTFD.683139.B1 | 4.0 |

Table 7: A number of lost protons can be calculated as $\frac{I_{ring}-I_{dump}}{I_{ring}}$. I_{ring} denotes the bunch intensity measured in the ring, I_{ring} - in the beam dump. Two BCTs per beam (B1/B2) and per location (BCTFR.A6R4 & BCTFR.B6R4/BCTFD.683130 & BCTFD.683139) were taken into account.

| | | | |
|------|------------|--------------|--------------|
| B1H | | Dump | |
| | | BCTFD.683130 | BCTFD.683139 |
| Ring | BCTFR.A6R4 | 55% | - |
| | BCTFR.B6R4 | 52% | - |
| B1V | | Dump | |
| | | BCTFD.683130 | BCTFD.683139 |
| Ring | BCTFR.A6R4 | 16% | 63% |
| | BCTFR.B6R4 | 86% | 60% |
| B2H | | Dump | |
| | | BCTFD.683130 | BCTFD.683139 |
| Ring | BCTFR.A6R4 | - | 38% |
| | BCTFR.B6R4 | - | - |
| B2V | | Dump | |
| | | BCTFD.683130 | BCTFD.683139 |
| Ring | BCTFR.A6R4 | 17% | 28% |
| | BCTFR.B6R4 | - | - |

operation, the ADT is kept running to damp the beam oscillations but here the ADT was initially dis-activated to impose the same initial conditions for both, injection and nominal, energy tests. Moreover, the excitation was to occur after the initial beam size measurements. A pilot bunch with an intensity of $\approx 10^{10}$ protons was injected into the LHC. After the injection oscillations were damped naturally, the Wire Scanner (WS) measurements were taken in both planes. The results are presented in Tab. 2. Each data set consists of two values: σ_{in} , taken when the wire goes through the beam, and σ_{out} - when the wire returns to its parking position. Usually, the average value σ_{avg} is used for analysis. Next, the ADT was activated which resulted in beam excitation and was followed by losses on the collimators. This procedure was repeated for all four cases.

The ADTs were used as the source of the beam disturbance and collimators played role of the targets. Detailed information on the elements used during the MD is given in Tab. 3. The longitudinal positions of the ADTs, TCPs and BLMs are presented in Tab. 4. Tab. 5 contains the exact timing of the beam dumps and the initial bunch intensities based on the Post Mortem records.

The LHC ring is equipped with two redundant Fast Beam Current Transformers (FBCT) per beam measuring bunch intensities. In the LHC the "B" system used to be developed but "A" system should be operational as well. Also two FBCTs per beam are installed in the beam dump[6]. The beam intensity measurements in the beam dump allow us to estimate in the first approach the number of the particles which were lost on the collimators². A comparison of the assembled data is given in Tab. 6. Measurements of two monitors per beam and per location are presented depending on the data availability. A value of $\frac{I_{ring}-I_{dump}}{I_{ring}}$ defines the number of particles lost on the collimators since no significant losses were observed along the ring (Tab. 7). Nevertheless these results are subject to considerable uncertainty since the FBCT measurements are strongly dependent on the beam position[7].

Although the Direct Current Current Transformers (DCCT) provide the most reliable intensity measurements with high precision (an error less than 1%), their sensitivity is insufficient for low intensity beams. Therefore they could not be used here.

3.2 Experiment at nominal energy (4 TeV)

In terms of machine protection, the 4 TeV part was much more critical than the 450 GeV test and a simple extrapolation of the injection results could not be applied to foresee the loss structure and location. The impact of the phase advance was not fully understood at this time and losses in the ARC regions had to be avoided so as to not quench any magnet accidentally.

The beams could be excited and damped separately. Thus, both beams were injected to the LHC and ramped to 4 TeV. Each beam consisted of ten pilot bunches with bunch spacing greater than $1 \mu s$ (the injection scheme: MD_MK1.13inj_both). Single bunches were excited independently with the increasing ADT gain. The initial plan of the experiment is presented on Fig. 5. In terms of the collimation system, only one target jaw of the primary collimator (TCP) was retracted to the position of the secondary collimator jaws (6.3σ). The other jaw was left at 4.3σ (Fig. 6 and Tab. 8). Beam 2 was supposed to be excited first in the horizontal plane and, depending on the results, beam 1 could be used afterwards.

Contrary to the test at 450 GeV, here the change of the BLM Monitor Factors could not be applied due to the operation with multibunches. The single bunch losses could result in

²This method can be used only if no losses occur elsewhere. Otherwise additional corrections must be taken into account.

extraction of entire beam from the accelerator. The BLM UFO Buster was used for the data acquisition. The Study Buffer is ≈ 3.5 s long but the data could be recorded only within 350 ms. The difference between Post Mortem and BLM UFO Buster buffers is explained in Section 4.9. The timing tables were used for a synchronization of the BLM UFO Buster and the BPM bunch-by-bunch data acquisition with the ADT excitation.

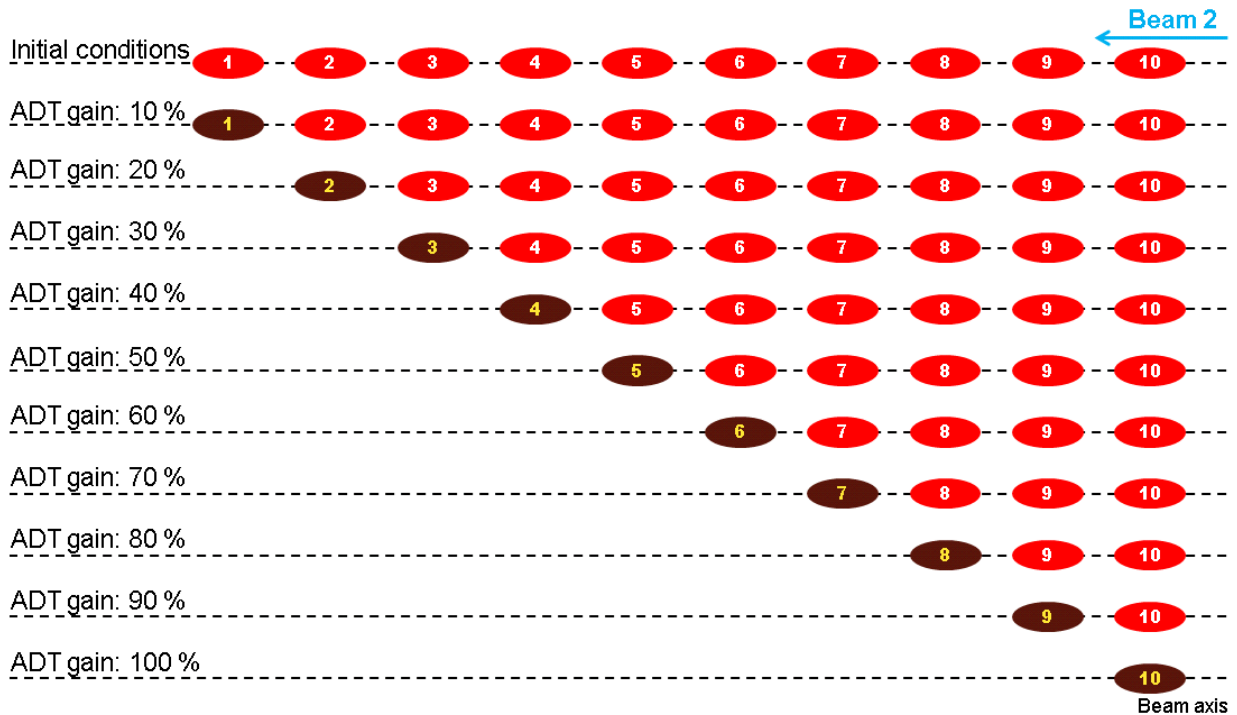


Figure 5: An excitation of the bunches. The single bunches were excited with increasing by 10% ADT gain.

Table 8: The collimator settings at 4 TeV. All dimensions given in millimeters. σ_{nom} corresponds to nominal σ , BB stands for the beam based center, J_L - left jaw (upper), J_R - right (lower) jaw.

| Target half gap | | | | | Initial settings | | Beam 2 |
|-----------------|-------|-------------|-----------|----------------|------------------|--------------|--------------|
| | | | | | 4.3σ | 4.3σ | 6.3σ |
| Beam | Plane | Collimator | BB centre | σ_{nom} | J_L | J_R | J_R |
| 1 | Hor | TCP.C6L7.B1 | -0.178 | 0.351 | 1.333 | -1.689 | -2.392 |
| 1 | Ver | TCP.D6L7.B1 | 0.240 | 0.253 | 1.330 | -0.850 | -1.357 |
| 2 | Hor | TCP.C6R7.B2 | 0.520 | 0.351 | 2.031 | -0.991 | -1.694 |
| 2 | Ver | TCP.D6R7.B2 | 0.770 | 0.253 | 1.860 | -0.320 | -0.827 |

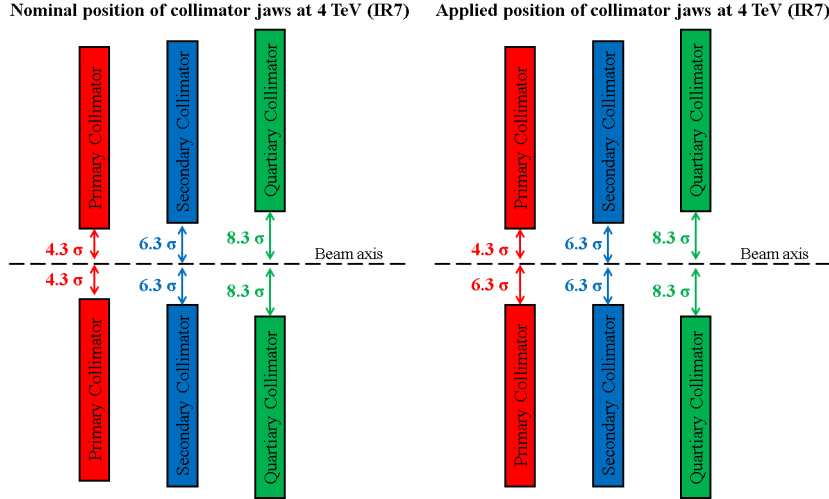


Figure 6: A scheme of the collimators configuration for 4 TeV beam. Left picture: the nominal settings, right picture: the applied modifications (not to scale).

4 Results and discussion

4.1 Beam loss temporal distribution

The UFOs are characterized by a sudden increase of the beam losses with the Gaussian temporal distribution with σ of about 1 ms. Thus, a similar temporal loss distribution of induced losses was required. The results of the 450 GeV test are presented on Fig. 7. The losses were normalized per proton since the bunch intensities were not constant for all configurations of the beams and the planes. B1H denotes beam 1 excited in the horizontal plane, B1V corresponds to beam 1 excited in the vertical plane etc. A comparison of the peak losses showed that the excitation in the horizontal plane caused losses approximately three times larger (2.9 in the case of beam 1 and 3.4 in the case of beam 2) than in the vertical plane. These properties are related to the locations of ADTs along the ring (β -functions) and a quality of the amplifiers (see Section 4.3). Moreover, B2H represents slightly better properties than B1H in terms of a quantity of the initial losses.

4.2 BLM signal vs BPM signal at 450 GeV

A combination of the BPM Post Mortem data with the LHC steering program (YASP) has been used to derive the transverse beam positions at the location of the collimators since no monitors are installed there. BLM and BPM systems have different resolution - BLMs collect data every 40 μ s while BPMs - every LHC revolution (89 μ s). Since they are not synchronized to each other, a moment of the beam dump was used for the synchronization (Fig. 8). The green dotted lines represent the positions of the collimator jaws with respect to the beam center. The values of $\sigma_{nominal}$ are different for the horizontal ($\sigma_H=1.048$ mm) and vertical ($\sigma_V=0.756$ mm) planes. The most efficient beam excitation occurs for B2H resulting in the highest beam amplitude (≈ 5 mm) and the smallest time constant, i.e. the rise time which characterize the response of the beam to the applied ADT-induced excitation. In the case of the vertical excitations, the saturation level was reached. A magnification of the previous plots is given on Fig. 9. The orange dotted lines represent the beam positions $\pm\sigma_{avg}$ which are based on the wire scans (Tab. 2). The positions of the beam amplitudes mostly

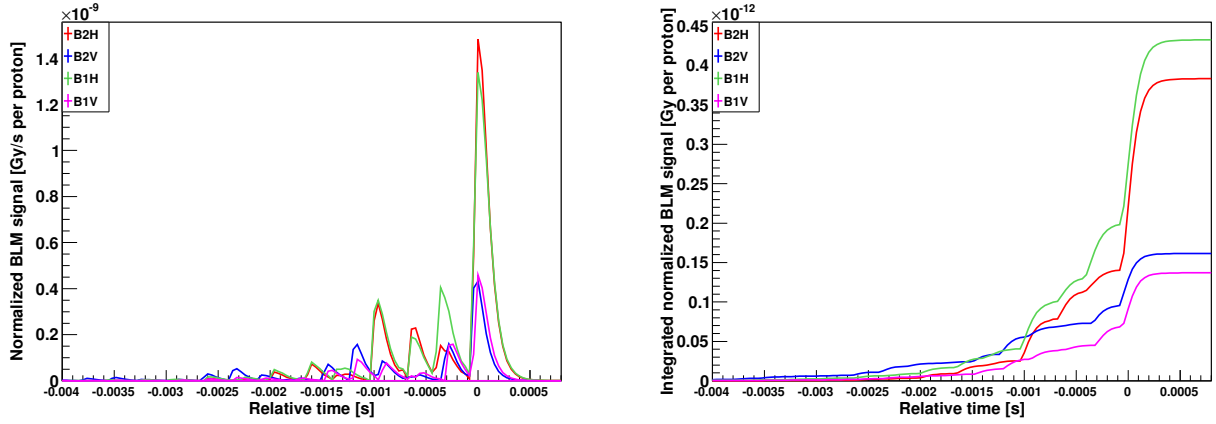


Figure 7: A temporal distribution of the ADT-induced losses at 450 GeV (left plot) and the integrated signals (right plot). B1H corresponds to beam 1 excited in the horizontal plane, B1V - to beam 1 excited in the vertical plane; the analogical abbreviations for beam 2.

correlate with the locations of the peak values of the BLM signals. However, the ratios are not conserved. For instant, in the case of B2H the one before last maximum BPM record corresponds to the BLM signal much smaller than the neighboring ones. Concerning B2V, even though the last five beam amplitudes stay on the similar level of about 2 mm, the BLM signals vary between ≈ 1 Gy/s and ≈ 4 Gy/s.

There is no uniform criteria for the synchronization of BPM and BLM systems. The presented method is commonly used but might contain an error of up to 2-3 LHC turns. Therefore, a method based on the sample correlation coefficient, which allows estimation of the linear dependency of two series of measurements, is proposed.

First of all, the BLM dataset was limited to a number of BPM measurement points. These BLM records were chosen which were the closest in the timescale to the BPM signals. The correlation coefficient is defined as [8]:

$$r_{x_{BPM}, y_{BLM}} = \frac{\sum_{i=1}^n (x_{BPM_i} - \bar{x}_{BPM})(y_{BLM_i} - \bar{y}_{BLM})}{\sqrt{\sum_{i=1}^n (x_{BPM_i} - \bar{x}_{BPM})^2 (y_{BLM_i} - \bar{y}_{BLM})^2}}$$

where x_{BPM_i} and y_{BLM_i} are measured values, \bar{x}_{BPM} and \bar{y}_{BLM} are the means of BPM and BLM samples, correspondingly. The values of $r_{x_{BPM}, y_{BLM}}$ are in the range of (-1,1). The positive correlation ($r_{x_{BPM}, y_{BLM}}=1$) represents increasing linear relationship between variables while the negative correlation ($r_{x_{BPM}, y_{BLM}}=-1$) shows a decreasing linear dependency. The largest value of $r_{x_{BPM}, y_{BLM}}$ indicates the most linearly correlated synchronization between BLM and BPM systems (Fig. 11).

Fig. 10 contains calculated values of $r_{x_{BPM}, y_{BLM}}$ depending on the time shift between two systems. Zero on x-axis corresponds to the synchronization to the moment of the beam dump.

The linear function

$$y_{BLM} = p_0 \cdot x_{BPM} + p_1$$

was fitted to the positive ($x_{BPM} > 0$) and the negative ($x_{BPM} < 0$) values of abscissa for the maximum correlation coefficients (Fig. 12). Mostly (three cases out of four), the positive BPM values are correlated linearly with the BPM signals.

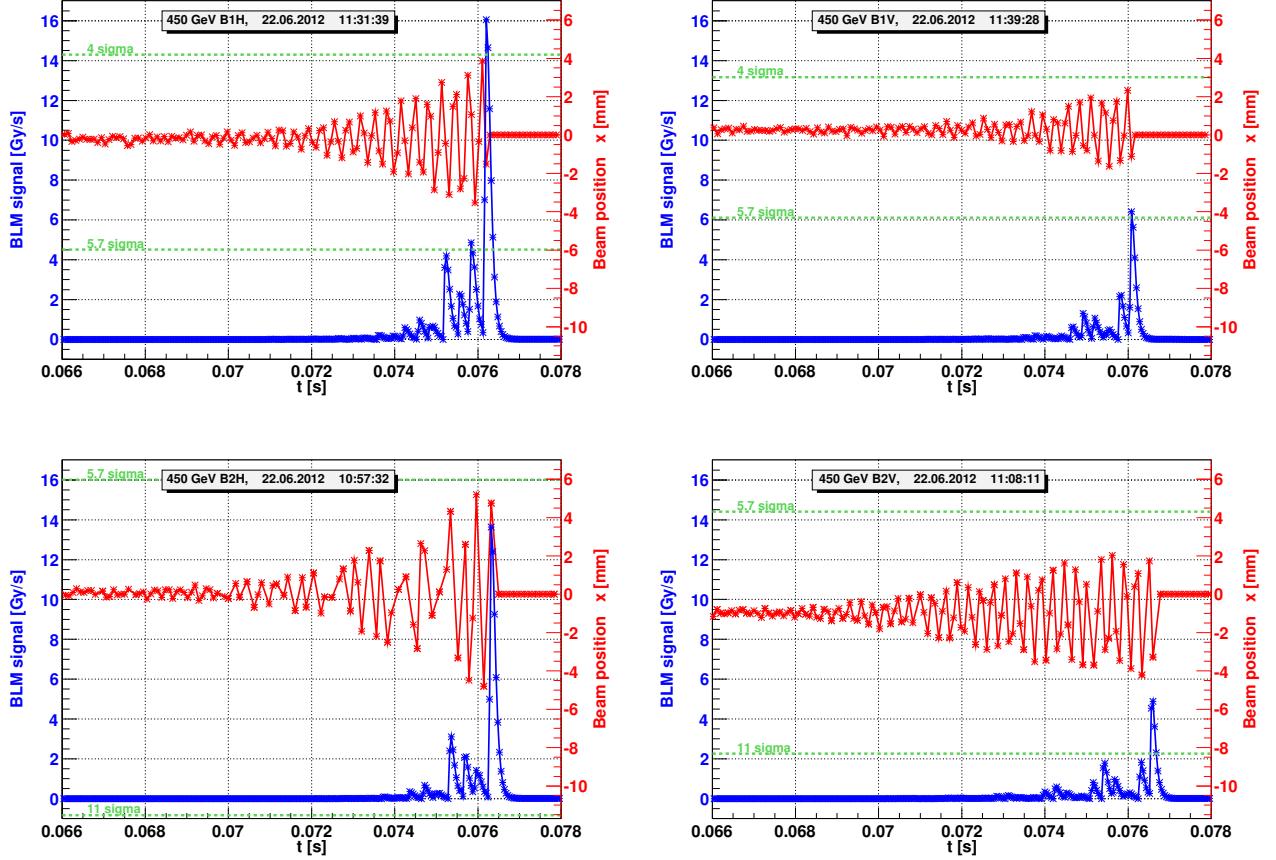


Figure 8: The beam oscillations compared to the loss distributions. Energy: 450 GeV. Upper plots present results for beam 1, the lower plots - for beam 2. The right part is related to the horizontal plane of the excitation and the left part - to the vertical excitation plane.

Table 9: Correlation coefficients between BLM and BPM signals.

| Case | Shift [turns] | Fit range [mm] | Parameter | Positive fit (right) | Positive fit (right) |
|------|---------------|----------------|-----------|----------------------|----------------------|
| B1H | 1 | (-4,4) | p0 | 1.81 ± 0.21 | -0.34 ± 0.11 |
| | | | p1 | -0.29 ± 0.20 | 0.02 ± 0.07 |
| B1V | 0.5 | (-2,2) | p0 | 0.45 ± 0.04 | -0.44 ± 0.14 |
| | | | p1 | -0.10 ± 0.02 | 0.05 ± 0.07 |
| B2H | 1 | (-6,6) | p0 | 0.77 ± 0.07 | -0.04 ± 0.02 |
| | | | p1 | -0.15 ± 0.08 | 0.03 ± 0.02 |
| B2V | -2 | (-4,4) | p0 | -0.04 ± 0.30 | 0.05 ± 0.04 |
| | | | p1 | 0.50 ± 0.25 | 0.16 ± 0.06 |

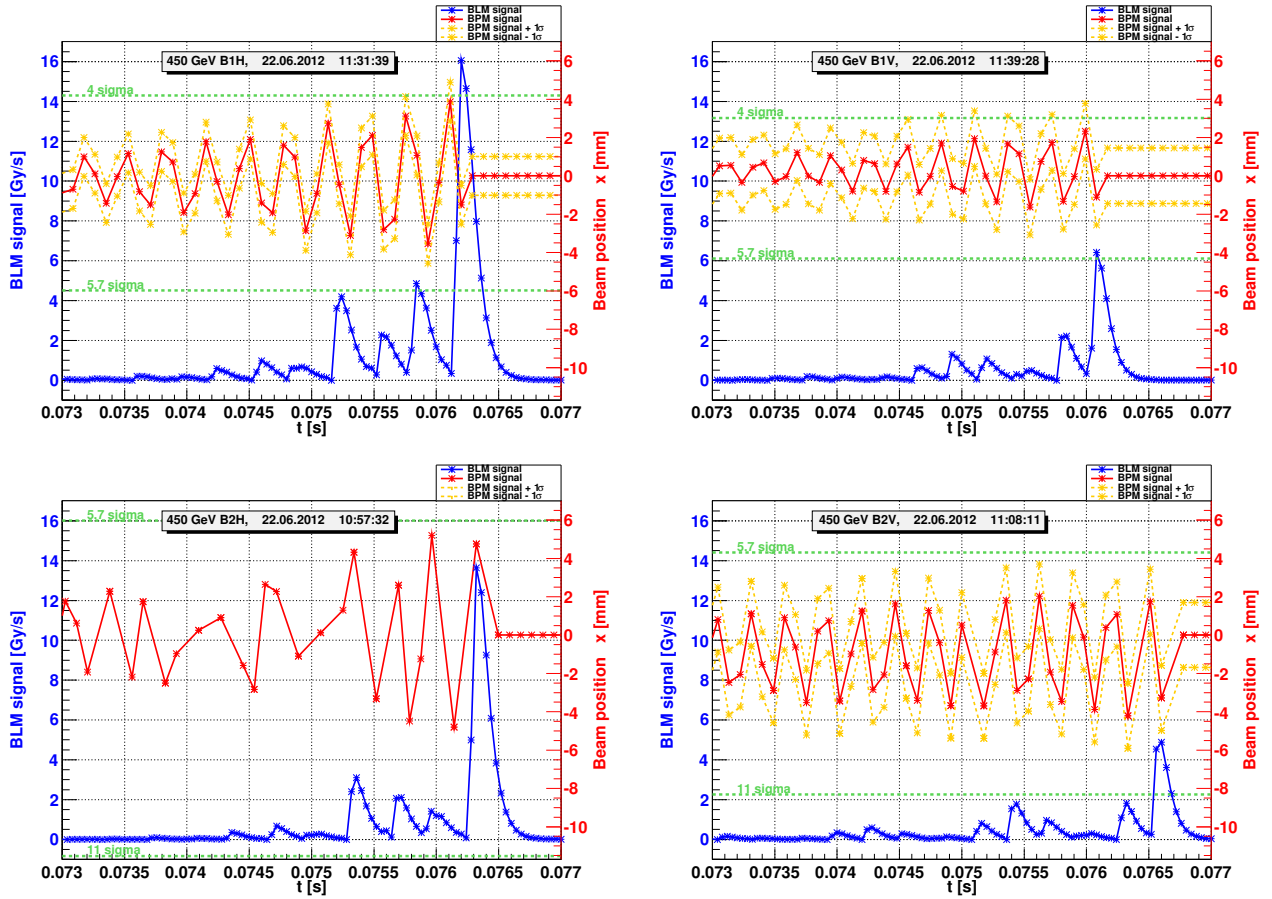


Figure 9: The beam oscillations compared to the loss distribution - a magnification of Fig. 8 with $\pm 1\sigma$ BPM signals. The data of B2H is missing.

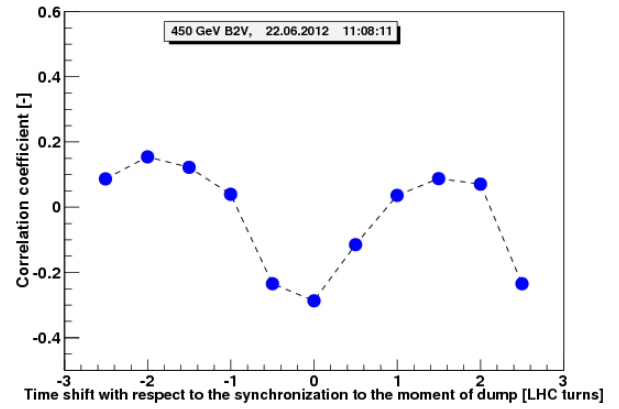
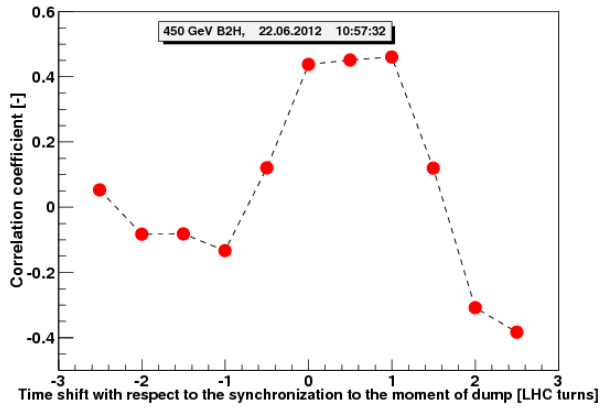
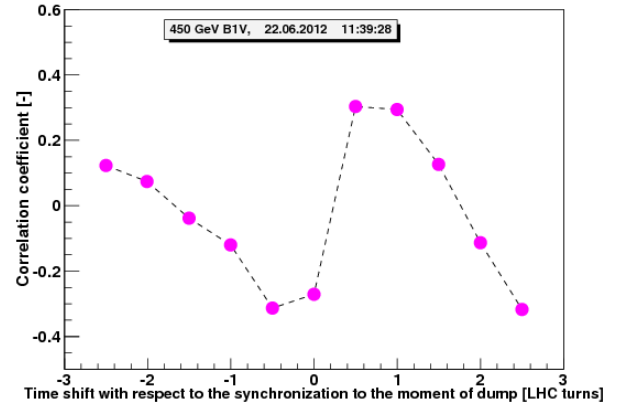
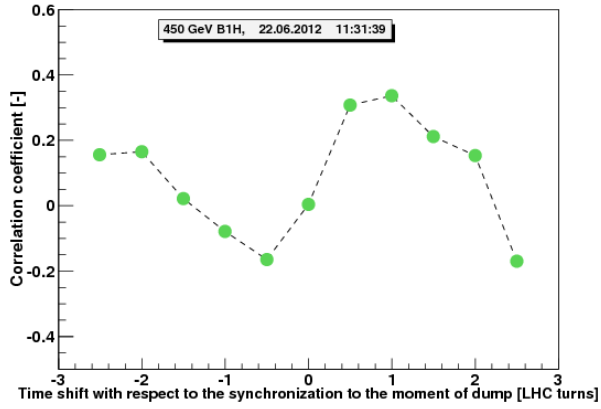


Figure 10: Correlation coefficients as a function of time shift between the BLM and BPM systems. Description in the text.

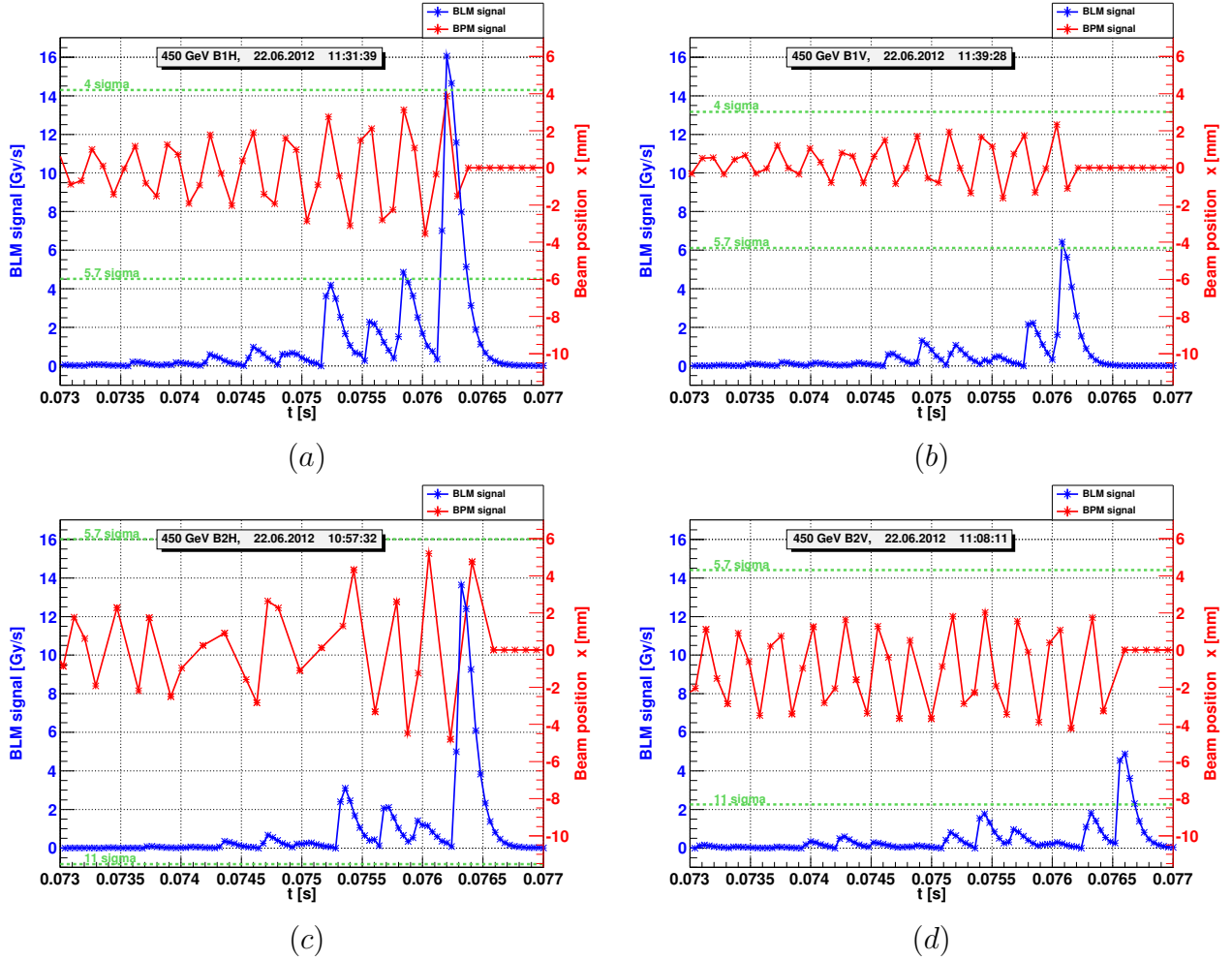


Figure 11: The BLM signals compared to the BPM measurements. The synchronization between the systems was based on the maximum value of the correlation coefficient. *a*) - shift by +1 LHC turn, *b*) - shift by +0.5 LHC turn, *c*) - shift by +1 LHC turn, *d*) - shift by -2 LHC turns.

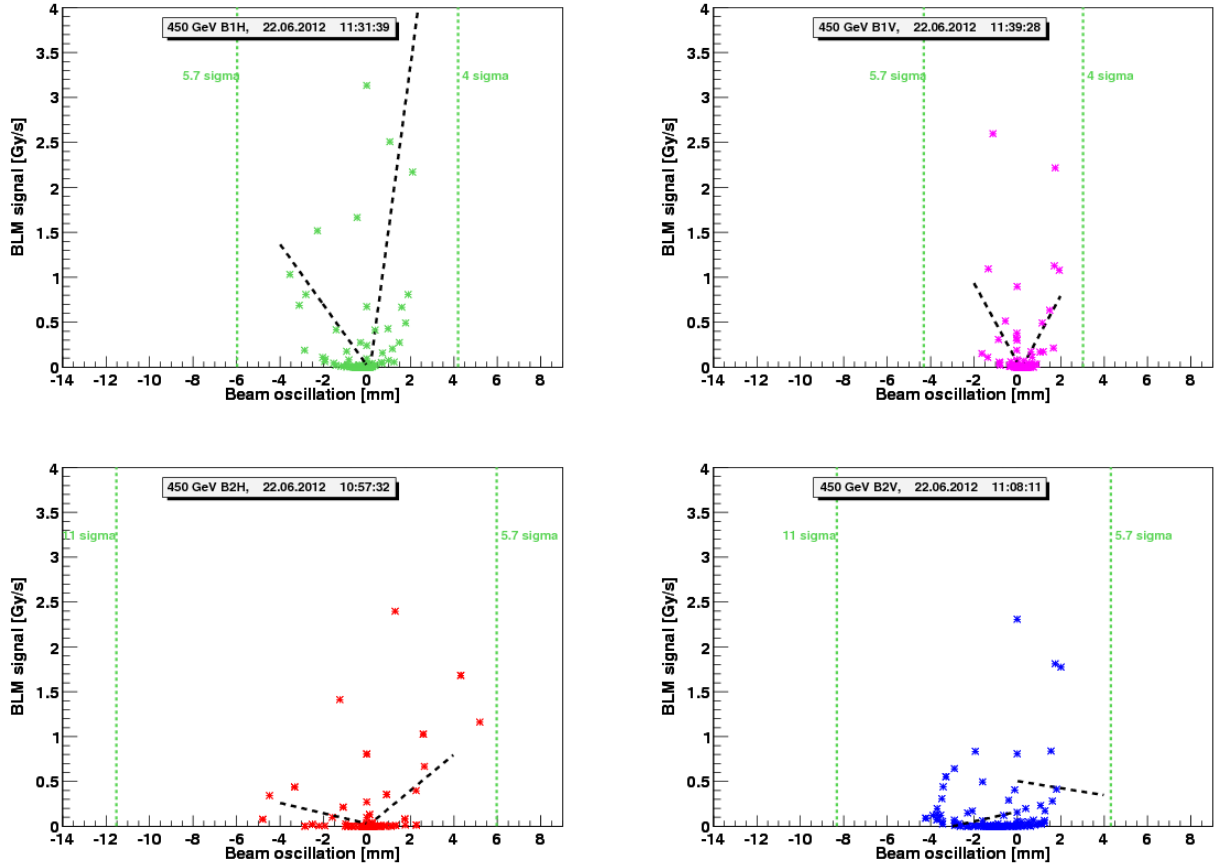


Figure 12: The BLM signal as a function of the beam oscillations. The black dotted lines represent separate fit functions for the positive and the negative values of BPMs.

Table 10: The β -functions at the locations of the Transverse Damper. Source: jmad, model: LHC (LSA) 2011.

| ADT | β_x [m] | β_y [m] |
|---------------|---------------|---------------|
| ADTKH.A5L4.B1 | 248.938 | 99.975 |
| ADTKV.A5R4.B1 | 191.918 | 155.021 |
| ADTKH.A5R4.B2 | 199.017 | 241.123 |
| ADTKV.A5L4.B2 | 139.262 | 301.872 |

Table 11: The β -functions at the locations of the Primary Collimators. Source: jmad, model: LHC (LSA) 2011.

| TCP | β_x [m] | β_y [m] |
|-------------|---------------|---------------|
| TCP.C6L7.B1 | 150.529 | 82.763 |
| TCP.D6L7.B1 | 158.871 | 78.263 |
| TCP.C6R7.B2 | 150.529 | 82.763 |
| TCP.D6R7.B2 | 158.871 | 78.263 |

4.3 ADT excitation efficiency

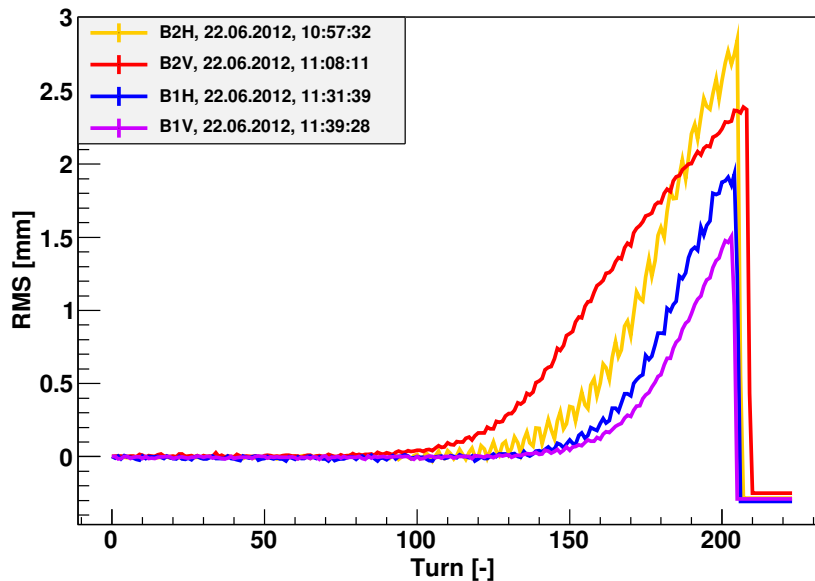


Figure 13: A comparison of the Post Mortem RMS of the arc BPMs. The LHC revolution period is $89 \mu\text{s}$. About 205 LHC turns before the beam dump are shown.

The ADT excitation efficiency depends mainly on two aspects:

- A physical condition of the ADT power amplifiers. Since the tubes of ADTKH.A5R4.B2 were changed several weeks before the MD, the excitation of beam 2 in the horizontal plane should be the most efficient.
- β -function at the position of the Transverse Damper (Tab. 10; for comparison the β -functions at the positions of the TCPs are given in Tab. 11). Therefore beam 2 in the vertical plane should be excited the fastest.

A comparison of the RMS of the LHC arc BPMs (Fig. 13) shows that indeed beam 2 is excited the most efficiently. Although B2V excitation starts earlier, B2H case is preferable due to the steep increase in the beam amplitude (the smallest time constant).

4.4 Impact of the phase advance

The impact of the phase advance between the source of the beam disturbance (the ADT) and the target (the collimator jaw) was investigated in terms of:

- Excitation efficiency
- Time structure
- Loss efficiency

In the LHC, the phase advances $\Delta\mu$ is defined with respect to the IP1 and increases clockwise. Therefore in the case of beam 1, the phase advance increases in the beam direction. In contrast, since beam 2 circulates anti-clockwise, the phase advance rises against the beam direction (see Fig. 14). Thus, the phase advance between ADT and TCP is calculated as follows:

a) for beam 1:

$$\Delta\mu_{ADT \rightarrow TCP} = \mu_{TCP} - \mu_{ADT} \quad (1)$$

b) for beam 2:

$$\Delta\mu_{ADT \rightarrow TCP} = \mu_{ADT} + (Q - \mu_{TCP}) \quad (2)$$

where Q is the tune defined as the number of betatron oscillations in one revolution turn:

$$Q = \oint \frac{ds}{\beta(s)} \quad (3)$$

The typical LHC working point has the horizontal tune $Q_x=64.26$ and the vertical tune $Q_y=59.31$. The results of the phase advance calculations for both beams and both excitation planes are given in Tab. 12.

Table 12: Phase advance between ADTs and TCPs. Since 0 rad is equivalent to 2π rad, only decimal parts are relevant in the conversion to degrees. The integer part has the meaning of the number of full (transverse) beam oscillations.

| Beam | Elements | Horizontal plane [2π] | Vertical plane [2π] | Horizontal plane [deg] | Vertical plane [deg] |
|------|-----------------------|-----------------------------|---------------------------|------------------------|----------------------|
| 1 | ADT \rightarrow TCP | 23.02 | 21.25 | 7.2 | 90.0 |
| 2 | ADT \rightarrow TCP | 40.43 | 37.39 | 154.8 | 140.4 |

Loss efficiency

The normalized total beam losses $l_{normalized}$ per circulating proton are presented as a function of phase advance $\Delta\mu$ between the appropriate ADT and the corresponding TCP (Fig. 15). The experimental points (B1H, B1V, B2H, B2V) were fitted with an arbitrary sinus-like function:

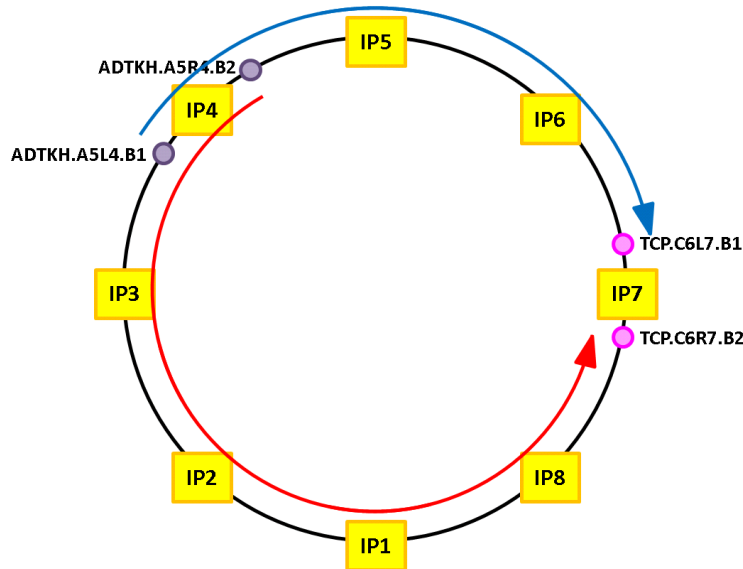


Figure 14: The phases μ for both beams are defined with respect to IP1 (Interaction Point 1 - ATLAS). Since beam 1 travels clockwise, the phase advance increases in the beam direction (the blue curve). In contrast, beam 2 circulates anti-clockwise so the phase advance increases against the beam direction (the red curve).

$$l_{normalized} = p_1 \left(1 - \frac{\sin(\Delta\mu)}{1.4} \right) \quad (4)$$

where $p_1=(1.67 \pm 0.12)$ and $p_2=1.4$ (assumed, fixed value) are the fit parameters.

The conclusion, based on these considerations, is that the highest loss efficiency occurs when the phase advance is close to 0 and π . As regards the loss efficiency, an operation at vicinity of $\Delta\mu = \frac{\pi}{2}$ should be avoided.

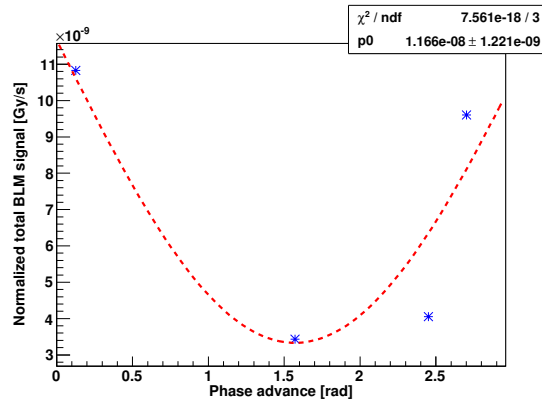


Figure 15: Normalized total losses as a function of phase advance between ADTs and TCPs.

Nevertheless, the level of the measured losses depends on many factors: an exact location and an orientation of the installed BLMs, a distance between the ADT and the TCP, β -functions and the beam size. Moreover data of both beams and both directions were merged here.

BPMs along the arc

The phase advance impact on the losses appearing at the location of the collimators is not reliable due to the contributions coming from many other sources. It is assumed that if the phase advance does not play any role in the excitation rate, different BPMs in the arcs should provide the same data but shifted in time. Three BPMs with different phase advances (with respect to the ADT) were compared in three arc regions R2, R6, R8. The results are presented on Fig. 16. The BPM offsets were subtracted. Slight differences between the signals can be observed especially with the higher beam amplitudes. Nevertheless, an operation with such large beam divergences from the beam axis leads to the smaller BPM accuracy³.

Summing up, the phase advance should not have any significant impact on the beam loss amplitude and the raise time.

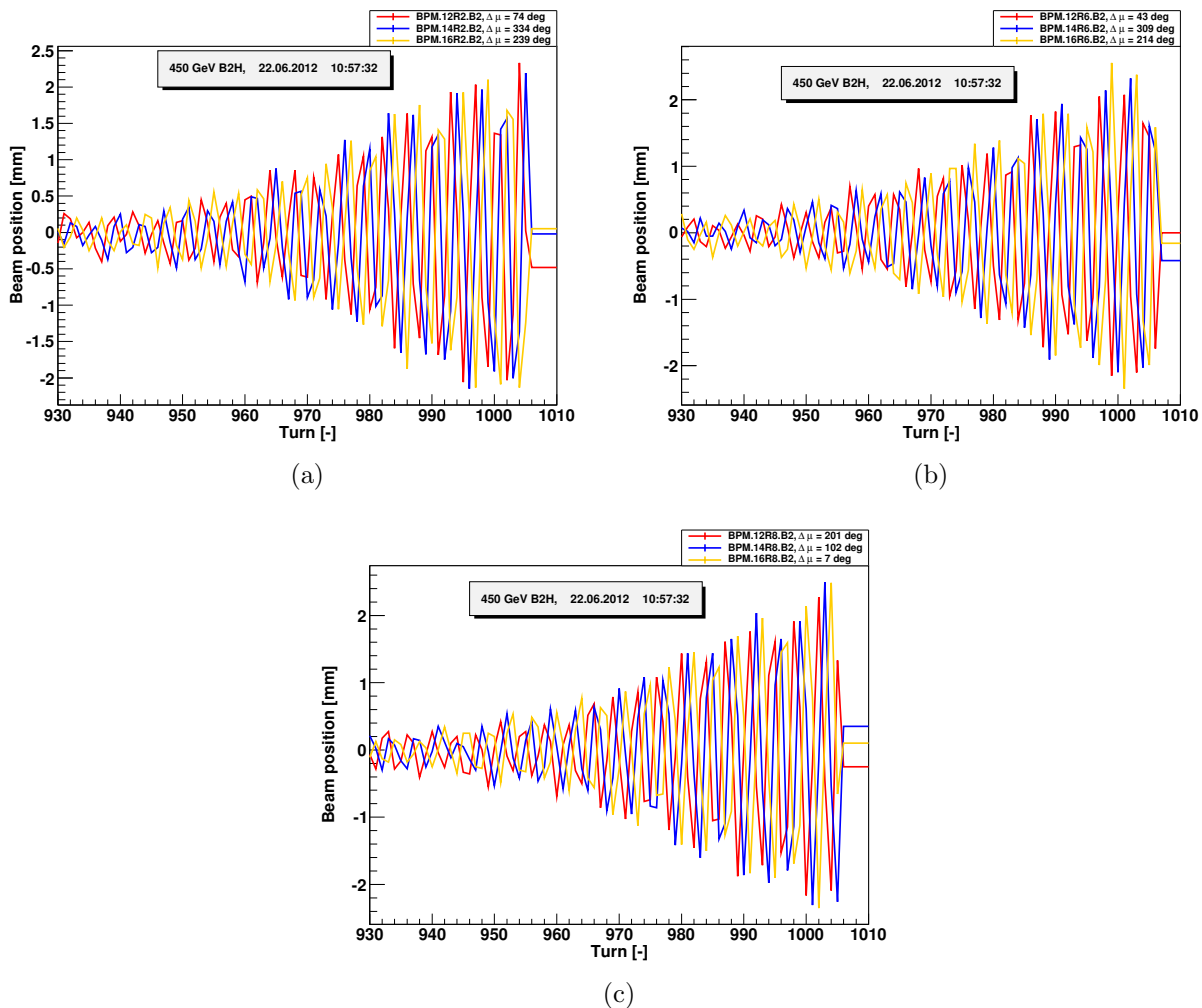


Figure 16: A comparison of the BPM measurements in R2 (a), R6 (b) and R8 (c).

³The accuracy of the beam position measurements depends mostly on a distance between BPM electrodes (Δw_{BPM}). A reasonable beam position margin is given by a standard deviation (δ_{BPM}) of 25% of Δw_{BPM} . Therefore, for the arc BPMs $\delta_{BPM} \cong 12$ mm and for LSS BPMs $\delta_{BPM} \cong 20$ mm [9].

4.5 Loss duration

A level of the BLM signal, at which a loss is considered to begin, is arbitrary. In the first approach it was assumed that the loss was continuous and greater than a certain factor. The loss duration was investigated with the factor changing from 1% to 10% of the maximum value of the B2H BLM normalized signal. The loss duration was studied as a function of the phase advance between ADTs and TCPs, a distance between them, the β -functions at the locations of ADTs and TCPs (Fig. 17).

Concerning the phase advance (Fig. 17a), the shortest loss duration is observed for the $\Delta\mu = \frac{\pi}{2}$ which corresponds to the case of B1V. The β -functions of TCPs are the same for beam 1 and beam 2 (Fig. 17b) in the corresponding places but the loss durations for the specific cases are different (26% when comparing B2V with B1V and 4% in case of B1H and B2H, blue stars considered).

The results depends to some extent on the assumed moment of the loss beginning. Therefore, the final conclusion is not straight forward.

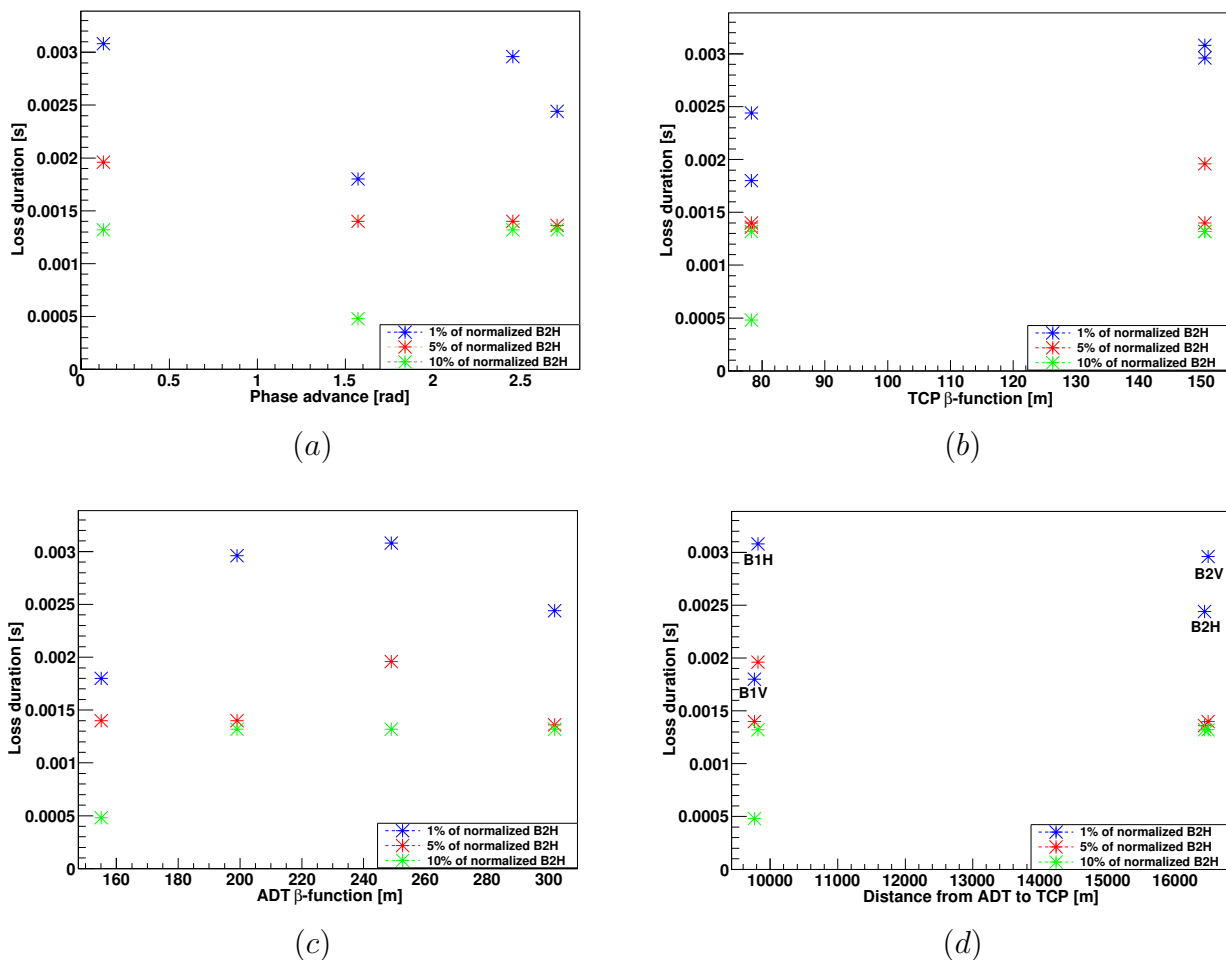


Figure 17: The loss duration as a function of the phase advance, β_{TCP} , β_{ADT} and a distance between ADT and TCP.

4.6 Beam transverse velocity

The beam transverse velocity averaged over a turn was simply calculated as:

$$\bar{v}_{transverse} = \frac{x_{n+1} - x_n}{t_{turn}} \quad (5)$$

where x corresponds to a beam transverse position and t is time between two records (89 μ s). Beam 2 excited in the horizontal plane reached the highest transverse velocity among all considered cases and gained the value of up to approximately $10 \frac{mm}{turn}$ which corresponds to $112 \frac{m}{s}$ (Fig. 18). While interpreting these plots one has to keep in mind that the initial conditions of the tests are unknown, i.e. the initial transverse position at the moment of the kick. Moreover the excitations are on top of the natural beam oscillations. These values are to illustrate how fast the beam can change its position within one turn.

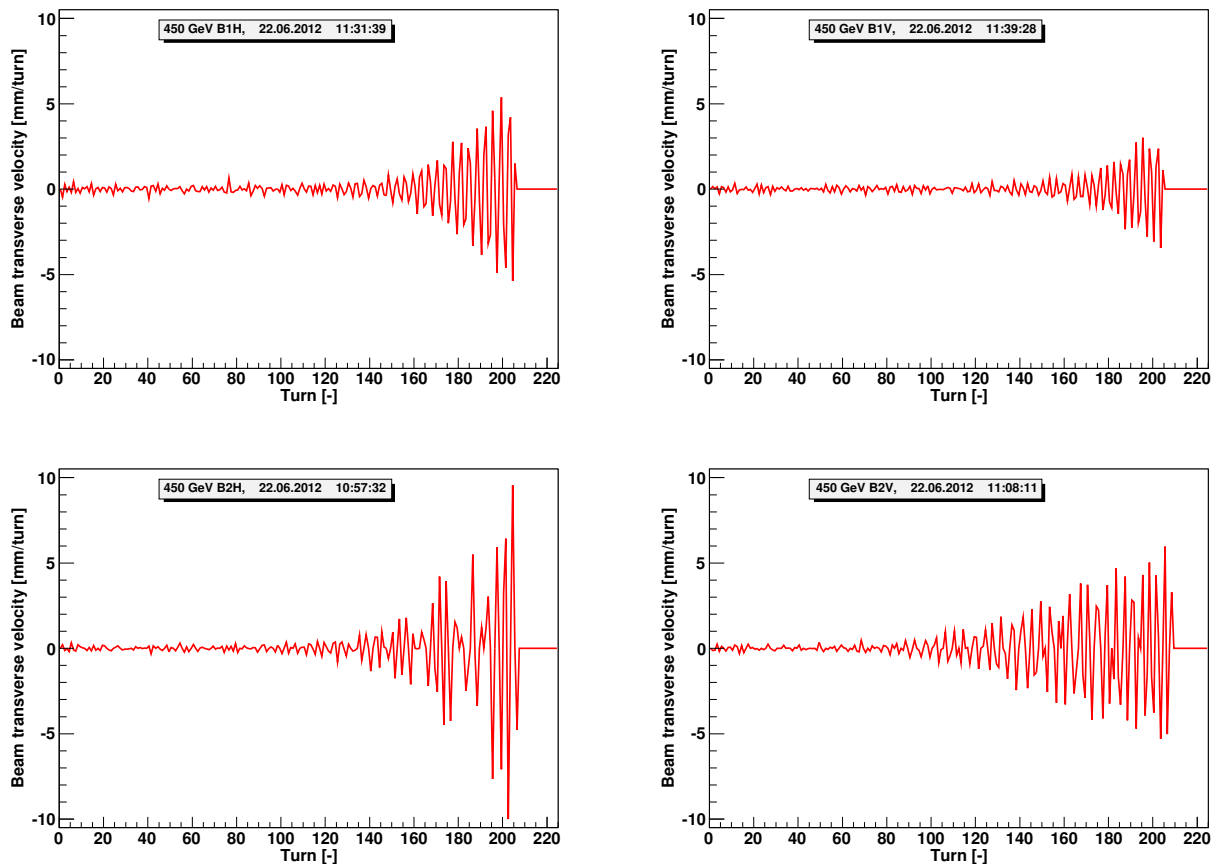


Figure 18: Beam transverse velocities.

4.7 Final results of ADT fast test at 450 GeV

Among many dependencies (the machine protection, the physical condition of the ADT amplifiers etc.), there are four the most important parameters determining the best candidate for the future Quench Test:

- Beam loss duration (the shorter the better)

- Beam loss amplitude (the highest)
- Beam loss confinement (no losses beyond a particular region)

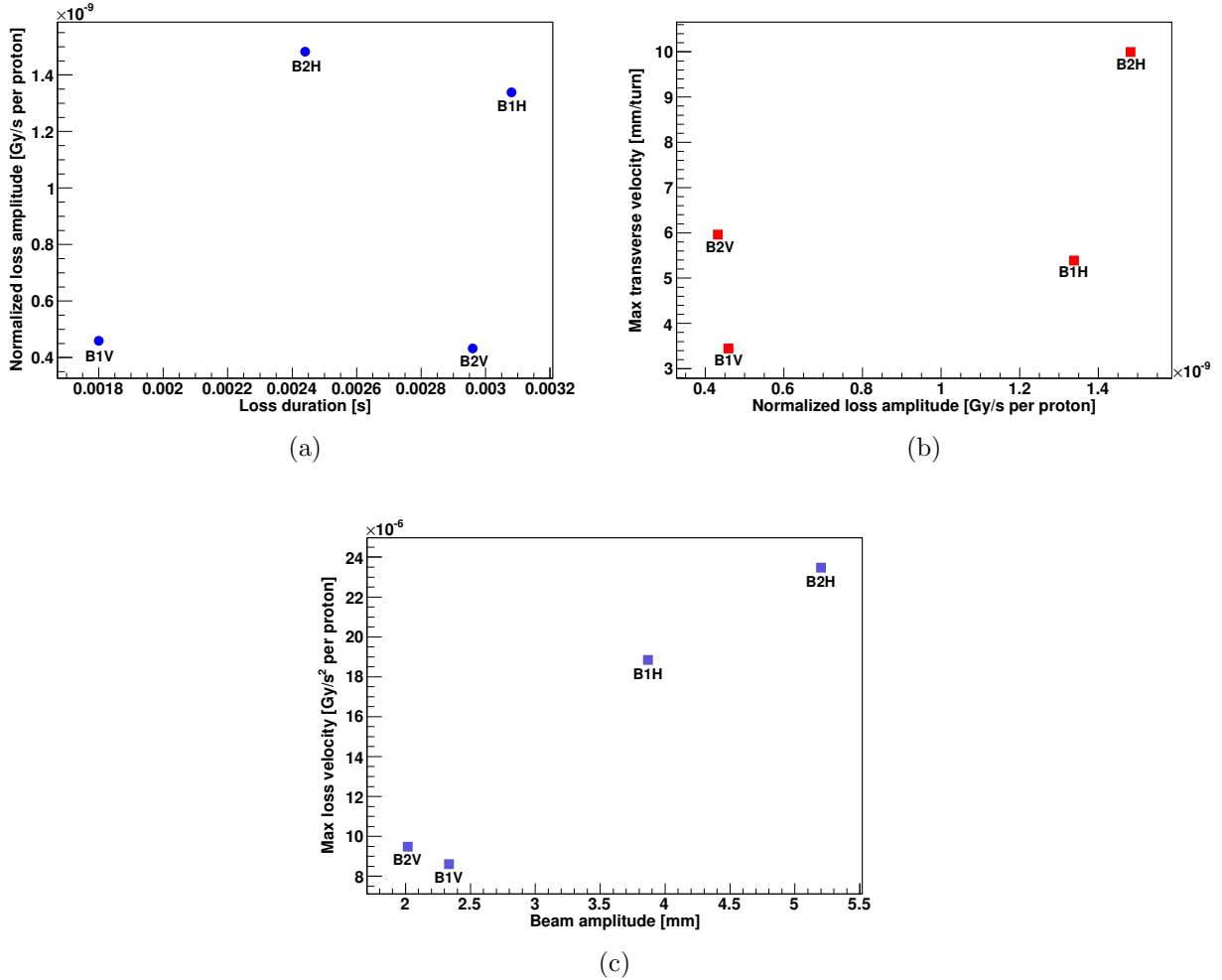


Figure 19: A combination of the final results: the loss duration and the normalized loss amplitude (a), the beam amplitude and the beam transverse velocity (b), the beam oscillation amplitude versus the loss velocity(c).

The normalized beam loss amplitude was presented as a function of the loss duration on Fig. 19a. Only the short loss duration is insufficient when the beam amplitude is low (B1V) but the combination of these two makes B2H the optimal candidate. The considerations of the maximum beam traverse velocity with respect to the normalized beam loss amplitudes (Fig. 19b) and a combination of the maximum beam oscillation amplitudes with the maximum loss velocities (time derivatives over BLM signal, (Fig. 19 c)) confirmed this statement as well.

4.8 ADT beam excitation at 4 TeV

Due to the machine protection the 4 TeV experiment with the ADT-induced beam excitation was performed in a very conservative way and changes were applied in very little steps. The initial idea was to inject ten pilot bunches per beam and excite single bunches with the ADT

gain increasing by 10% (Fig. 5). It was already mentioned that beam 2 was safer in terms of good splices in the magnet interconnections (Sector 6-7) where the potential losses could occur. Therefore it was used first. Depending on the results of the beam 2 test, beam 1 could be used afterwards. It was decided to ramp both beams due to the time constraints (no time for two independent ramps). An operation with high intensity beams causes BLM cross-talk and may lead to the beam dump of both beam even though losses had been induced only by one of them. Nevertheless, during this experiment, the low intensity bunches were used ensuring a separate beam extraction from the accelerator. The independent beam dumping applies only if the cross-talk between the BLM monitors is insignificant⁴.

As expected, the beam excitation at nominal energy turned out to be more difficult and slower than at injection. An excitation at 40% gain resulted in the loss of approximately a half of a bunch intensity while 50% gain caused the loss of 75% of the initial number of protons. The 6th bunch was excited to 100% of the ADT gain giving no sufficient BLM signal to extract the beam from the accelerator. An additional manipulation in the ADT electronics (changes in the digital gain) allowed imposing higher levels of excitation (Fig. 20). At 200% (13:07:52, local time) the BLM system gave only a warning but at 400% of the ADT gain the monitor BLMEI.06R7.B1E10_TCLA.B6R7.B1 triggered the beam dump (13:09:49, 8th bunch).

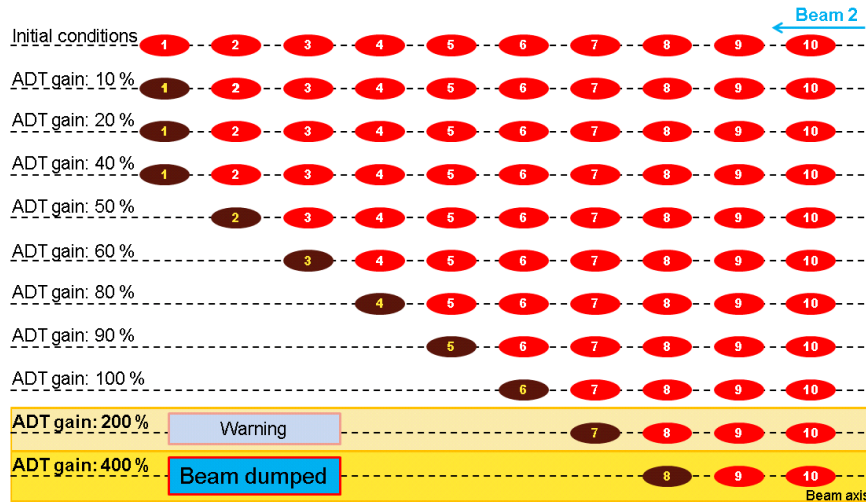


Figure 20: A scheme of the experiment. 4 TeV beam is rigid and therefore difficult to excite.

4.9 Bunch by bunch BLM data acquisition

Although eight bunches out of ten were excited, the BLM UFO Buster recorded only four of them. As it was already mentioned, this BLM system has 3.5-second long buffer but only 10% could be saved. A comparison of the Post Mortem (PM) and UFO BLM Buster buffers is given in Fig. 21. During the operation, the synchronization between the ADT and the BLM UFO Buster was applied. The losses at smaller ADT gains were slower than expected and did not fit to the set time window of the Study Buffer (300 ms).

Fig. 22 shows radiation doses at TCP.C6R7.B2 originating from the ADT single bunch excitations. The signals were normalized per proton. An increase in the ADT gain results

⁴Due to the scattering of the lost beam and the hadronic shower propagation, the losses can be seen not only by the monitors devoted for this beam but also by the monitors surveying the opposite beam. This effect is called the cross-talk and is a limitation for an independent beam dumping.

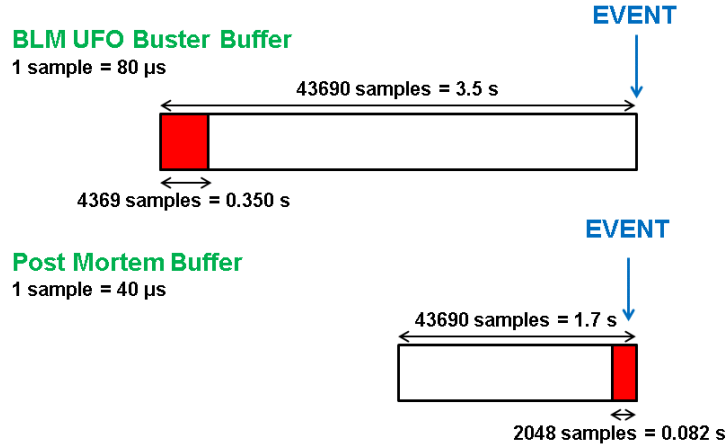


Figure 21: Comparison of the Post Mortem (PM) and BLM UFO Buster buffers. Both buffers contain 43690 samples but they differ in the sample length. The BLM UFO Buster buffer is 80 μ s long and the PM buffer is 40 μ s long. Moreover, when an event occurs, the data is recorded at the beginning of the buffer in the case of the BLM UFO Buster (first 10% of the samples). The PM data acquisition consists of two parts: before (\approx 78 ms) and after (4 ms) the event. The second component provides information on the beam extraction from the machine. More information can be found in [10].

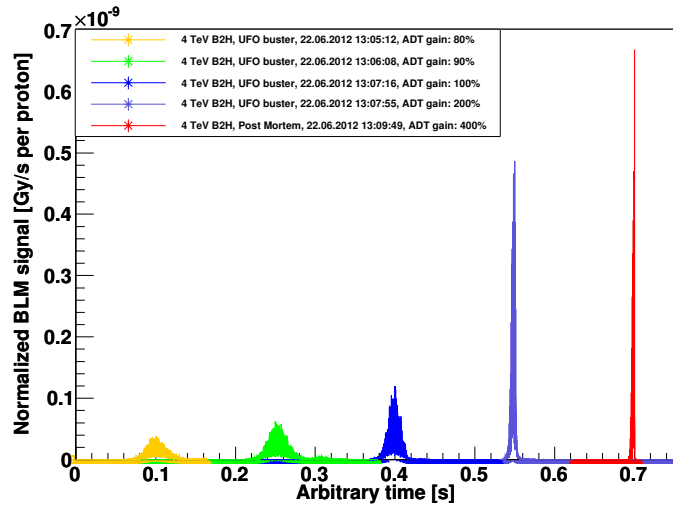


Figure 22: The losses induced by the single excited bunches at 4 TeV at TCP.C6R7.B2. An increase in the excitation results not only in the higher loss rate but also changes the loss shape. The BLM signal given by the beam excited to 400 % of the ADT gain (red line) is characterized by the most narrow distribution. First four distributions come from BLM UFO Buster, the last one from the Post Mortem.

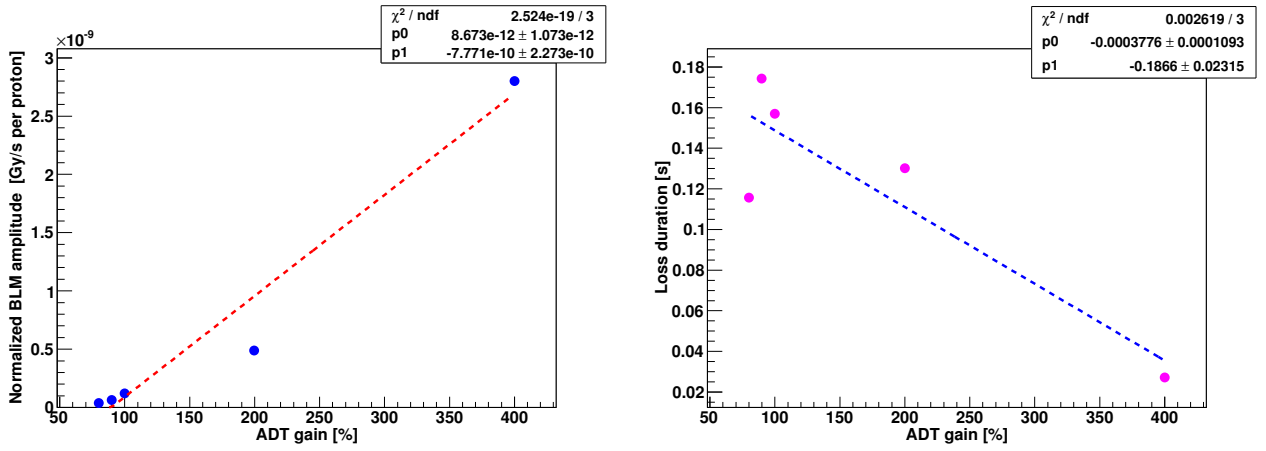


Figure 23: The ADT gain impact on the loss amplitude (the left plot) and the loss duration (the right plot) in case of the 4 TeV beam.

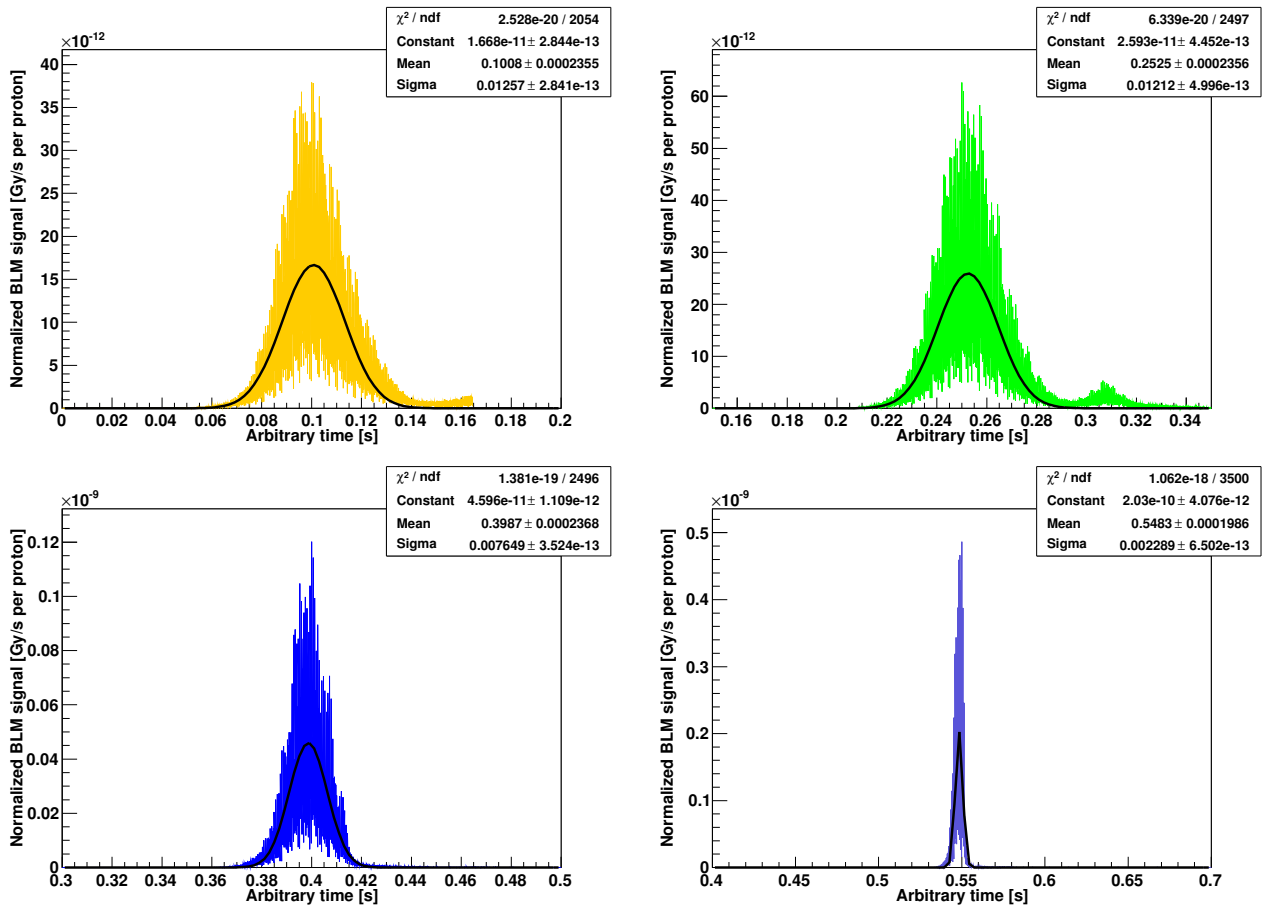


Figure 24: BLM signals of the beam excited at 80% (top left), 90% (top right), 100% (bottom left) and 200% (bottom right) of the ADT gain. The measured signals were fitted to the Gaussian distributions (black curves).

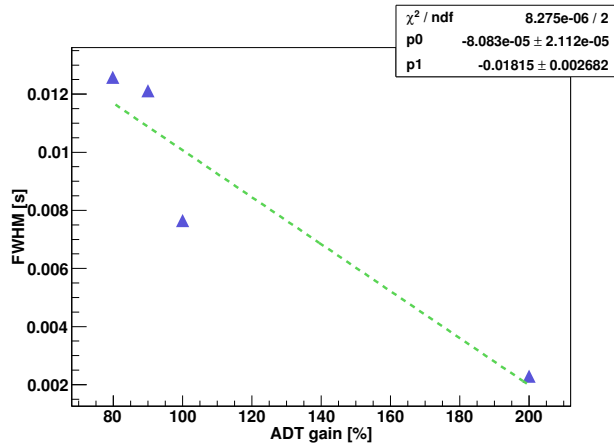


Figure 25: FWHM as a function of the ADT gain.

not only in a rise of the loss rate but also in the change of the distribution width. In this timescale the complex structure of the losses is not visible. The highest and the most narrow loss occurred for 400% of ADT gain (red line). The loss duration for this case is around 7 ms. The loss amplitude is a linear function of the ADT gain (Fig. 23, left plot). The bunch by bunch data acquisition allowed the studies of a correlation between the loss duration and the applied ADT gain since all excitations were performed for the same beam (2) and plane (horizontal). The right picture of Fig. 23 shows that the higher the ADT gain is, the faster losses are.

The first four signals were fitted to the Gaussian distribution (Fig. 24). The BLM records at 400% of the ADT gain were omitted since the excitation was not fully suppressed. The full width at half maximum (FWHM) can be calculated with the dependence given below:

$$\text{FWHM} = 2\sqrt{2 \ln 2} \sigma \approx 2.3548200 \sigma. \quad (6)$$

Here σ denotes the standard deviation. The results were illustrated as a function of the ADT gain and fitted to a linear function (Fig. 25).

4.10 BLM signal vs BPM signal at 4 TeV

The BPM bunch by bunch data acquisition collected the signal of the particle oscillations only for one bunch (7th bunch no. 1695, ADT excitation: 200%, 13:07:55). In this case the interpolation to the position of the TCP can not be done due to the incompatibility of the YASP and the BPM application output files. Therefore the readings of BPM.6R7.B2 is used for a comparison with the BLM signals at the TCP .

There are no uniform criteria of the time synchronization between these two system. The synchronization to the moment of the dump could not be used as previously since no dump happened at 200% of the ADT gain. Therefore, it was assumed that the signal maxima should occur close to each other. Fig. 26a indicates that although the beam excitation is gone, a decay of the BLM signal can be observed.

This approach was verified by the method presented in Section 4.2. The correlation coefficient reaches its highest value when the signals are shifted by nine turns with respect to the previously synchronized BLM and BPM maxima (Fig. 27). Fig. 26b is presented for comparison with Fig. 26a. Fig. 28 shows BLM signal as a function of BPM signal with linear

fits for positive and negative BLM values. Tab. 13 contains the details of fitting. Only in the case of the positive part of Fig. 28b the linear dependence was found.

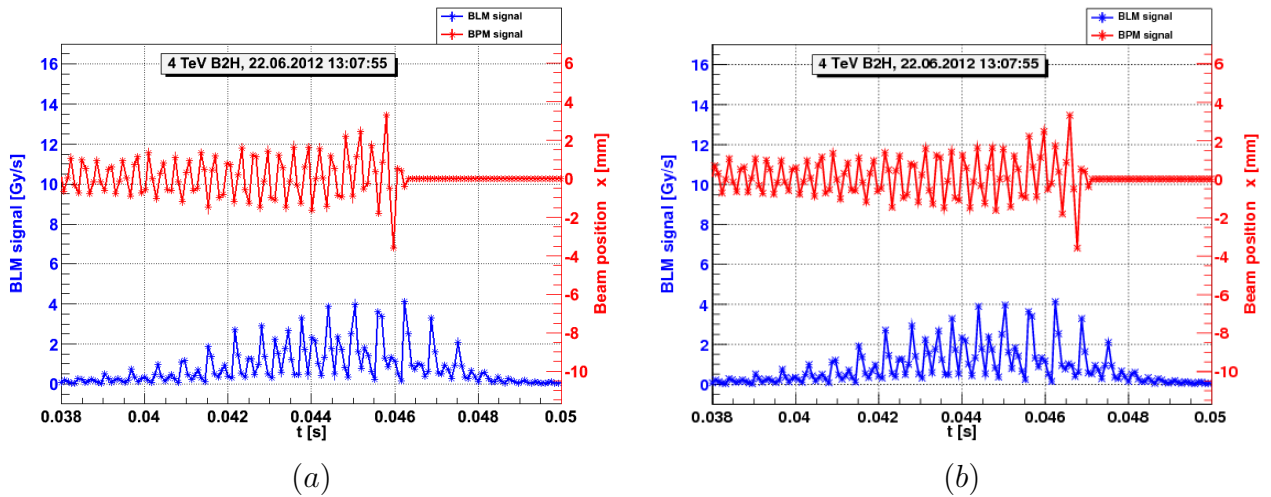


Figure 26: 4 TeV test: BLM and BPM signals after 200% of the ADT gain excitation. The left plot shows the synchronization to the maxima of both signals, the right plot presents synchronization based on the highest correlation coefficient calculated with Eq. 4.2.

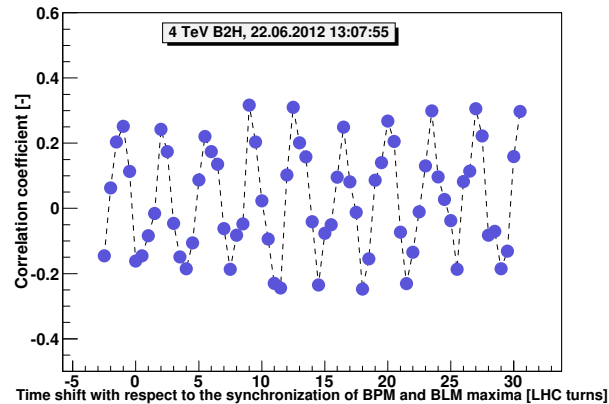


Figure 27: Correlation coefficients as a function of time shift between the BLM and BPM systems. The synchronization to maxima of BLM and BPM signals was used as the reference (zero on the x-axis). The highest value appears for the shift of nine turns.

4.11 Comparison of loss duration of UFOs, Wire Scanner-induced losses and ADT-induced losses

It was already mentioned that the UFOs are characterized by the losses in the order of 1 ms and the temporal loss distribution possesses the Gaussian shape. Fig. 29 presents three cases of 4 TeV LHC beam losses: the UFO, the Wire Scanner (WS) Quench Test [11] and the ADT fast losses test. There are three UFO events: the UFO event recorded on 13th May 2012 at 15:03:20 by the BLM UFO Buster and two UFOs which triggered the beam dump

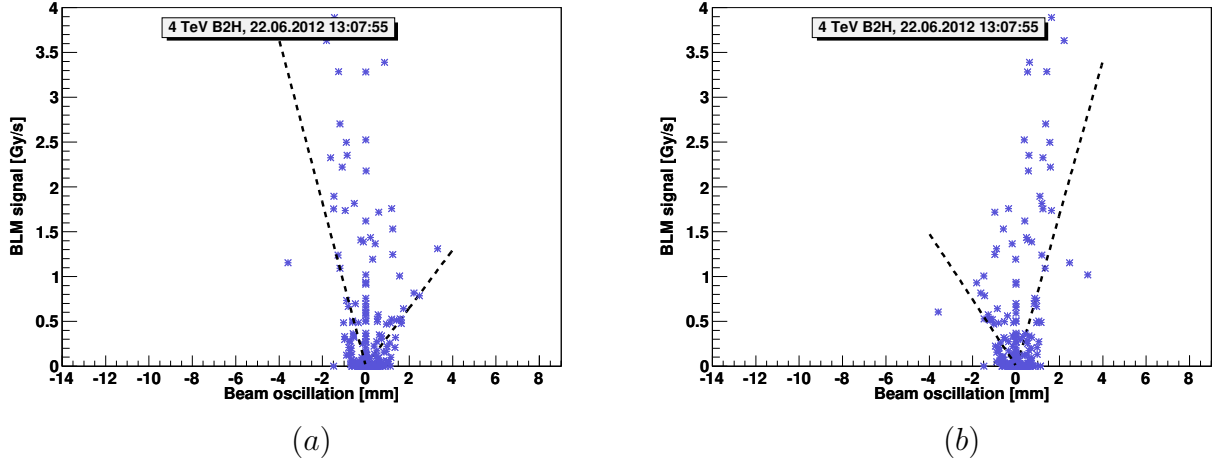


Figure 28: 4 TeV test: BLM and BPM signals after 200% of the ADT gain excitation. Left plot shows the synchronization to the maxima of both signals, right plot presents synchronization based on the highest correlation coefficient calculated with Eq. 4.2.

Table 13: Correlation coefficients between BLM and BPM signals in the case of 4 TeV bunch excited with 200% of the ADT gain.

| Case | Shift [turns] | Fit range [mm] | Parameter | Positive fit (right) | Positive fit (right) |
|------|---------------|----------------|-----------|----------------------|----------------------|
| B2H | 1 | (-4,4) | p0 | 0.3 ± 0.1 | -0.9 ± 0.2 |
| | | | p1 | 0.002 ± 0.030 | 0.003 ± 0.030 |
| | 9 | | p0 | 0.9 ± 0.1 | -0.4 ± 0.2 |
| | | | p1 | -0.03 ± 0.03 | 0.006 ± 0.030 |

(3rd August 2012 at 06:28:57 and 23rd August 2010 at 13:50:38). The experiment with the WS was done on 1st November 2010 at 15:40:03 with the wire velocity of $5 \frac{cm}{s}$ ⁵. The ADT part shows the data collected at 400% of the ADT gain (22.06.2012, 13:09:49). The ADT beam excitation resulted in beam losses around 7.5 times shorter in comparison with the 2010 Wire Scanner Quench Test but still around 7 times longer than UFOs.

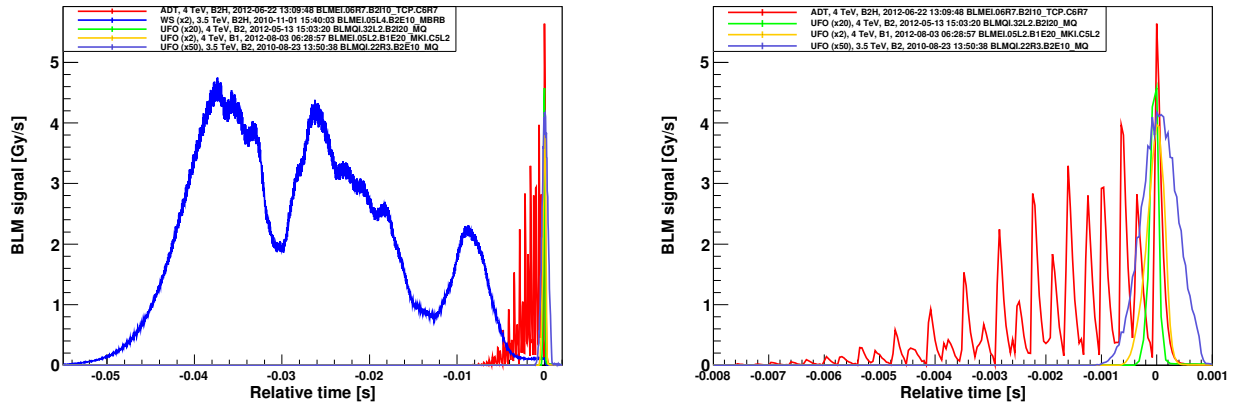


Figure 29: A comparison of 4 TeV LHC beam losses. The left plot: five cases are presented: three UFOs, ADT-induced losses and WS-induced losses. Signals were scaled by factors given in the table. The right plot: ADT-induced losses have a complex spiky structure consisting of peaks and gaps. The UFOs represent the Gaussian distribution shape.

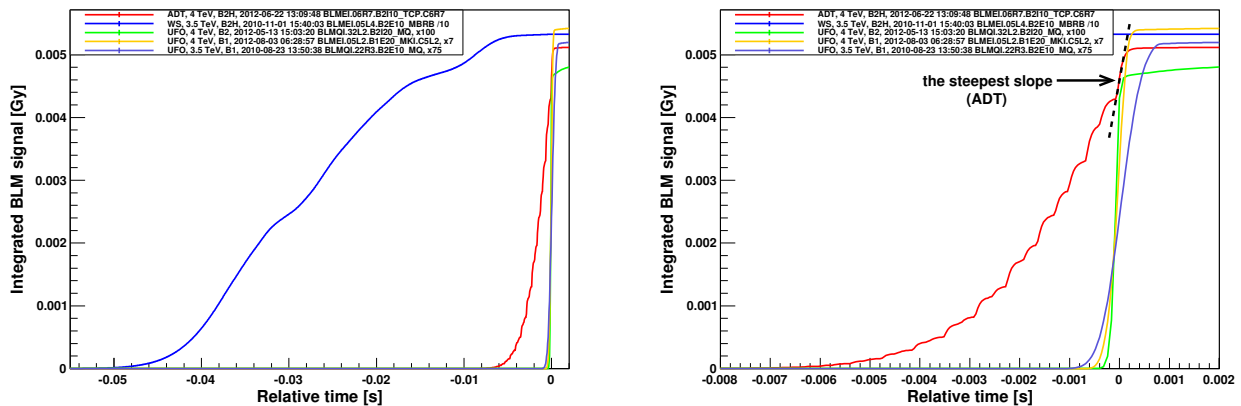


Figure 30: Integrated BLM signals.

An integration of the losses (Fig. 30) indicates that a certain region in the ADT case represents required properties - the increase is steep enough (a black dotted line) to simulate the UFO losses. The main problem is how to impose appropriate conditions, i.e. a beam deviation with respect to the axis center, during the Quench Test with the 3-corrector orbital bump.

⁵A repetition of this test was proposed with more beam intensity what could result with magnet quench at about $10 \frac{cm}{s}$. Nevertheless the proposal was rejected due to the worries about quenching MBRB magnet.

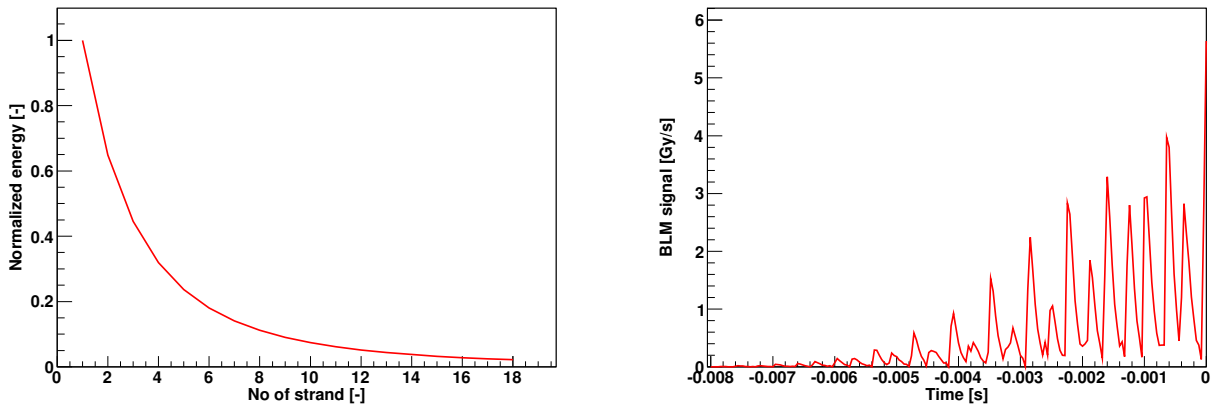


Figure 31: Inputs to the QP3 heat transfer code. The left plot shows the radial energy distribution along the superconducting coil (Geant4 simulations). The right plot presents the temporal loss distribution (experimental data).

4.12 Importance of the temporal loss shape for the final Quench Test

An energy level, at which a quench of the superconducting cables occurs, can be calculated with the QP3 heat transfer code [12]. A loss distribution in time, a radial energy distribution inside the superconducting coil, a magnet current (6374 A for 4 TeV, 177.08 A per a strand) and a loss duration are the main inputs to the program. An average energy E_{avg} is the most important output and has a meaning of the minimum quench energy (MQE). A comparison of the different loss distributions was done to determine how they affect the quench limit. During this MD no superconducting element was directly targeted by the beam (the losses on the collimators) and no magnets quenched. Therefore the values of E_{avg} are given only for comparison. Fig. 31 shows the QP3 input data. The radial energy distribution along the superconducting coil was taken from the Geant4 simulation[13],[14]. The temporal loss distribution comes from the ADT fast losses test at 4 TeV with 400% of the ADT gain.

Two cases were considered: the first one takes into account whole 7 ms range of the loss, the other one assumes that only last 0.12 ms (the last peak in the BLM signal) played role in quenching. Depending on the loss shape, for the 7 ms timescale the variations up to 40% were estimated. The results are presented in Tab. 14. The loss shape is unimportant for quenching. The integrated loss is the thing which matters[15].

4.13 Energy dependence on the loss rate and the beam excitation (B2H case)

Beam 2 was excited in the horizontal plane at 450 GeV and 4 TeV. Although the conditions of these two cases were different (see Tab. 15) the behaviour of the beam and the loss evolution can be compared.

Beam oscillations

The beam oscillations were compared at the same location of the Beam Position Monitor - BPM.6R7.B2. According to the collimator settings, only those of the transverse beam

Table 14: A comparison of the quench limits provoked by the different shape beam losses.

| Loss duration | Beam loss shape | $E_{avg}[mJ/cm^3]$ | $\frac{E_{avg}}{E_{avgBLM}}$ |
|---------------|---|--------------------|------------------------------|
| 7 ms | BLM signal shape (4 TeV, B2H, 400% ADT gain) | 9 | 1 |
| | Triangular | 11 | ≈ 1.3 |
| | Rectangular | 13 | ≈ 1.4 |
| | Linear | 10 | ≈ 1.1 |
| 0.12 ms | BLM signal shape, last peak only (4 TeV, B2H, 400% ADT gain) | 6 | 1 |
| | Triangular | | |
| | Rectangular | | |
| | Linear | | |

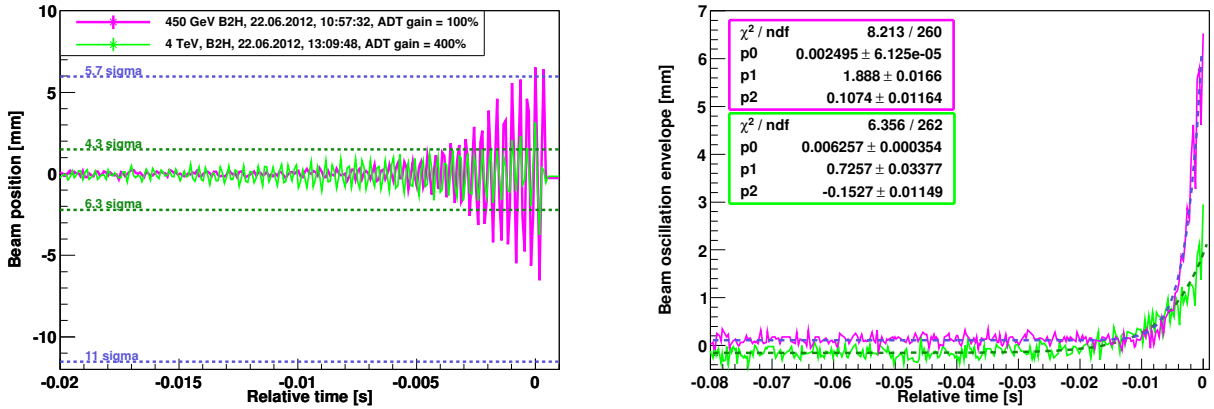


Figure 32: A comparison of the BPM signals at the location of BPM.6R7.B2 for 450 GeV (magenta line) and 4 TeV (green line). The dotted lines on the left plot represent positions of the collimator jaws (TCP.C6R7.B2) at 450 GeV (purple line) and 4 TeV (dark green line). On the right plot the beam envelopes were fitted to the exponential functions.

Table 15: A comparison of the conditions at 450 GeV and 4 TeV.

| | Energy [TeV] | $J_L[\sigma]$ | $J_R[\sigma]$ | ADT gain [%] | Beam intensity [protons] |
|-----|--------------|---------------|---------------|--------------|--------------------------|
| B2H | 0.45 | 5.7 | 11 | 100 | $9.2 \cdot 10^{10}$ |
| | 7 | 4.3 | 6.3 | 400 | $8.3 \cdot 10^{10}$ |

positions can be taken into account which are smaller than the aperture limitations (Fig. 32). The initial beam oscillations at 4 TeV are slightly larger than those at 450 GeV but it might result from 4 times larger ADT gain which was applied. Later, from around 5 ms before the beam dump, the 450 GeV beam amplitudes increase much faster than those at 4 TeV. An exponential function

$$x_{beam}(t) = Ae^{\frac{t}{\tau}} + b \quad (7)$$

was used to calculate the time constant τ ($p0$ on the plot), i.e. the rise time. This value characterizes the system response to an input which varies in time. A ($p1$) and b ($p2$) are the fit parameters. Parameter b has the meaning of the offset. The time constants for 450 GeV and 4 TeV beams are $\tau_{450GeV} = (2.50 \pm 0.01) \cdot 10^{-3}$ s and $\tau_{4TeV} = (6.30 \pm 0.03) \cdot 10^{-3}$ s, respectively.

Temporal loss distribution

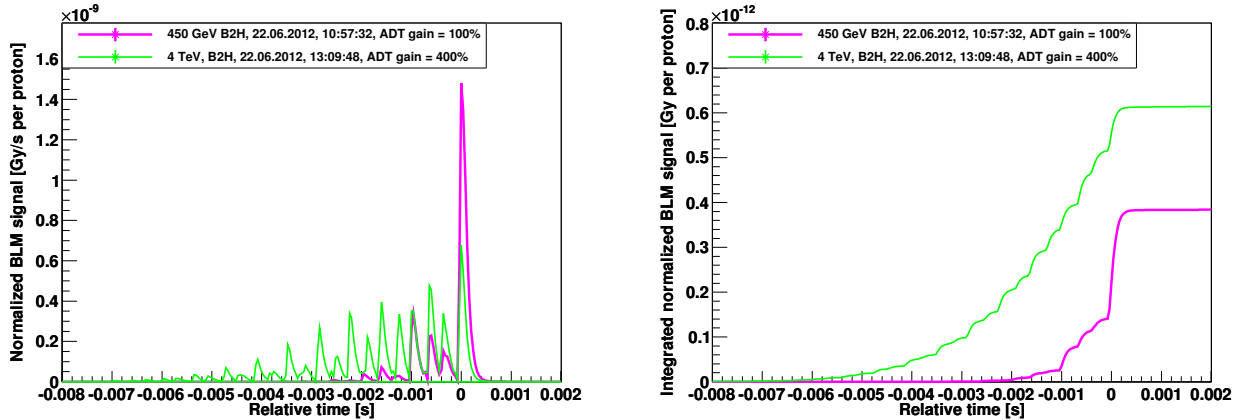


Figure 33: A comparison of the BLM signals (the left plot) and integrated signals (the right plot) at the location of TCPs (B2I10_TCP.C6R7.B2) for 450 GeV (magenta line) and 4 TeV (green line).

The temporal loss distributions were compared at the location of TCP (Fig. 33). In the case of 450 GeV beam, the loss is characterized by several relatively short initial losses which are followed by the high narrow peak. The situation for 4 TeV beam is different - the losses are built in the form of peaks and gaps between them but the loss envelope increases steadily. In terms of the loss duration, the losses at nominal energy are longer by a factor of 3 and the maximum is smaller approximately twice. Concerning the integrated signals, in the very last part, the slopes are pretty much the same.

4.14 Losses along the LHC ring

The losses occurring beyond a devoted region are always an issue as regards any beam-involved experiment. This is also crucial during the Quench Test planning since the beam has to be lost on a particular magnet.

Fig. 34 - Fig. 38 show the BLM signals along the LHC ring during the ADT fast losses test (1.3 s integration time). Most of the losses occurred in the region of collimators (Octant 7) where the aperture limitations were applied. No more significant losses were observed except the dump region.

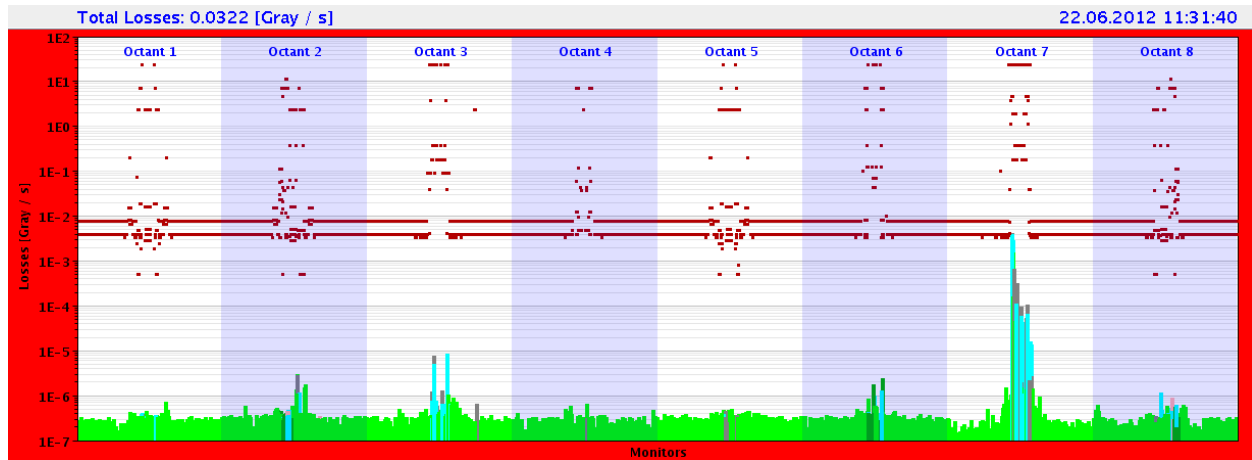


Figure 34: B1H, 450 GeV: losses along the LHC ring.

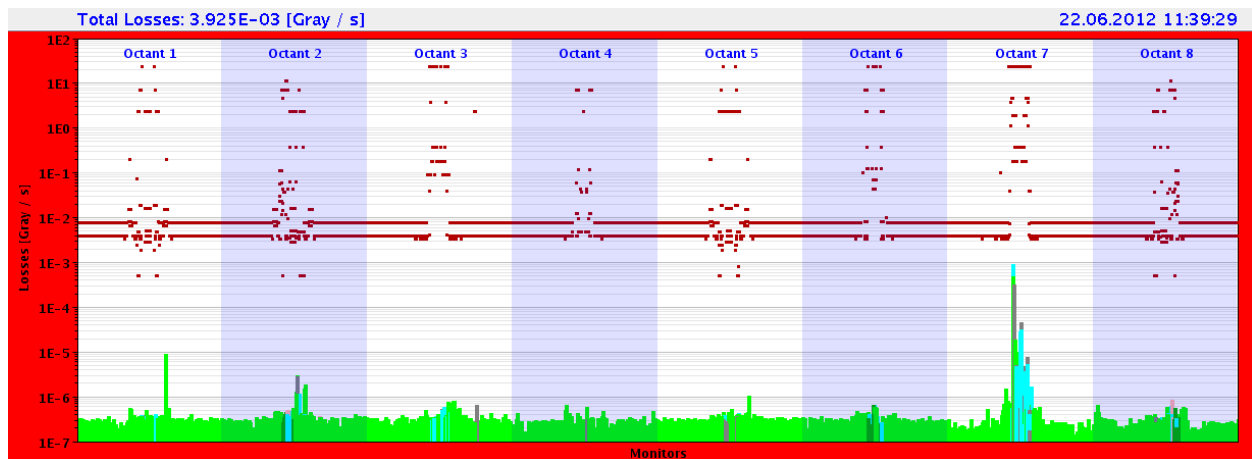


Figure 35: B1V, 450 GeV: losses along the LHC ring.

5 Summary and conclusions

The MD was performed successfully. All objectives were accomplished as planned. Due to the lack of time beam 1 at 4 TeV was not used. Nevertheless the results of beam 2 test were sufficient for our studies:

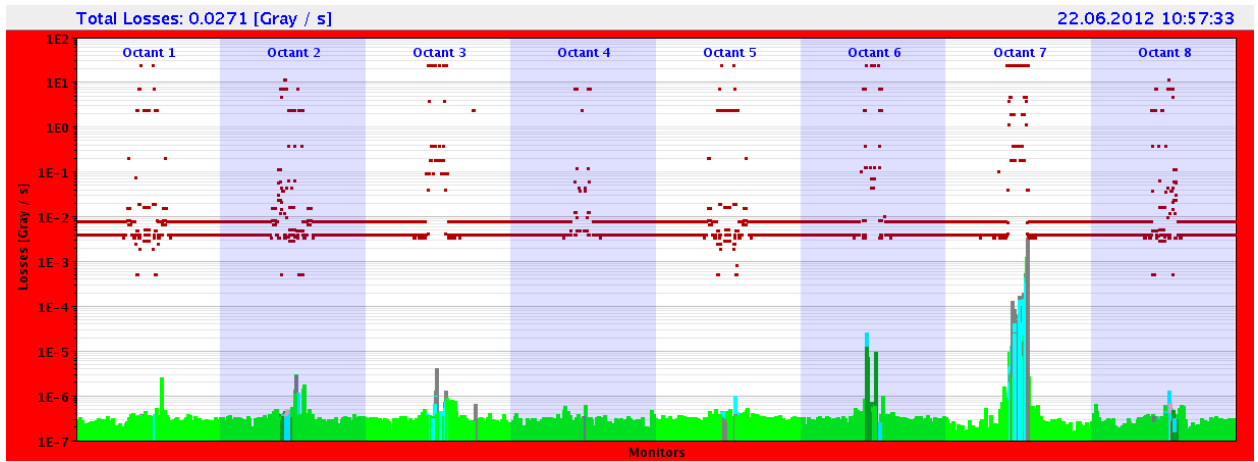


Figure 36: B2H, 450 GeV: losses along the LHC ring.

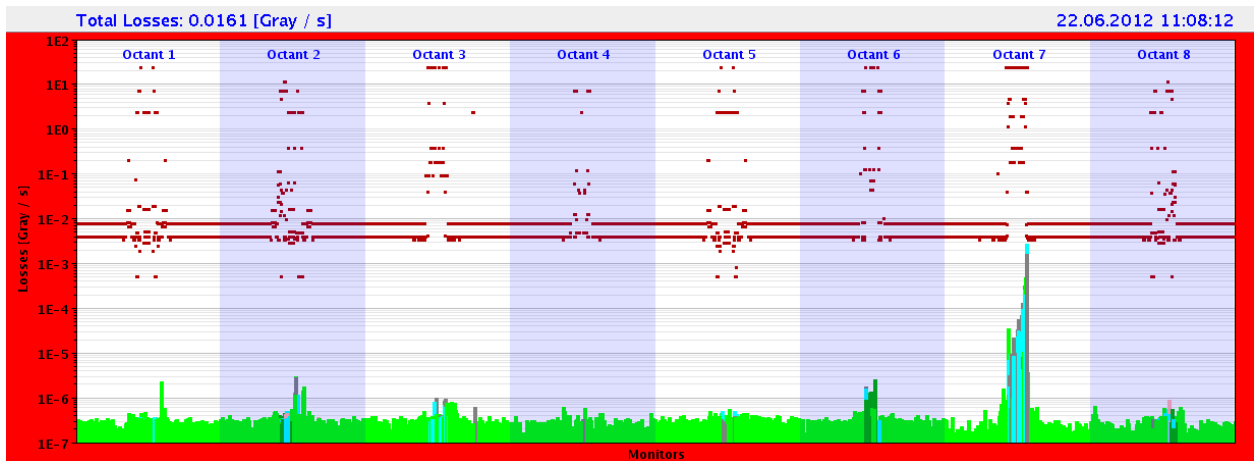


Figure 37: B2V, 450 GeV: losses along the LHC ring.

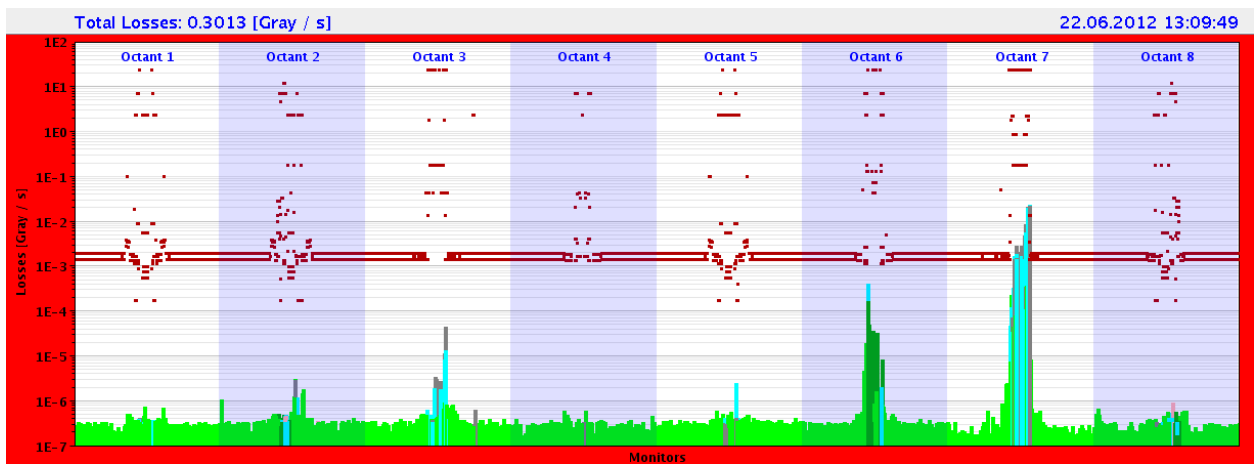


Figure 38: B2H, 4 TeV, 400% gain: losses along the LHC ring.

- The Transverse Damper was used in a non-standard way (the sign flip method) and well beyond its typical operational performance (400% of gain). The test not only approved the ADT as a system for the fast losses induction but also delivered important information about the worst case failure scenario.
- Beam 2 excited in the horizontal plane is proposed as the optimal candidate for the future Quench Tests. It is characterized by the most convenient properties among all the other options. Moreover, beam 2 is considered safer than beam 1. The result is also satisfying in terms of the excitation plane since the UFO-losses dominate in the horizontal plane[16].
- The phase advance might have impact on the beam losses but there are plenty of other factors contributing. The conclusions are not completely clear.
- The shortest obtained losses at 4 TeV are still seven times longer than UFOs. Nevertheless, thanks to the existence of the heat transfer models, these longer losses would provide conclusive results for the UFO timescale. The measurements of the longer losses could be extrapolated to a short loss scenario for the ADT.
- The details of temporal loss shape have small impact on the quench level.
- The losses were localized in the aperture limitations. No significant losses were observed except one monitor in B2H case.
- The ADT method of the beam excitation is good enough to be used during the Fast Losses Quench Test in winter 2013.

References

- [1] T. Baer *et al.*, "UFOs in the LHC", IPAC'11, TUPC137, Sept. 2011
- [2] A.Priebe, "ADT Fast Losses Test 25/25 March 2012", LHC Study Working Group meeting, 27.03.2012
- [3] A.Priebe, "Planning the ADT experiments", Quench Test Strategy Working Group meeting, 4.05.2012
- [4] M. Sapinski, "Proposal for Beam Induced Quench Tests at the end of 2013 run", LHC Machine Committee, 24.10.2012
- [5] Minutes of Quench Test Strategy Working group meeting, 16.03.2012 (<https://indico.cern.ch/conferenceDisplay.py?confId=182393>)
- [6] "LHC Design Report", Vol 1, Chapter 13: "Beam Instrumentation" (<http://lhc.web.cern.ch/lhc/lhc-designreport.html>)
- [7] Jean-Jacques Gras, private communication
- [8] A.K. Sharma, "Text book of Correlation and Regression", DPH Mathematics Series, 2005
- [9] Marek Gasior, private communication

- [10] BLMLHC: Beam Loss Monitors, <http://project-beam-instr-sw.web.cern.ch/project-beam-instr-sw/Welcome.php>
- [11] M. Sapinski *et al.*, "LHC magnet quench test with beam loss generated by wire scan" , IPAC'11, WEPC173, Sept. 2011.
- [12] A. Verweij, QP3: Users Manual, CERN/EDMS 1150045
- [13] A. Priebe, Geant4 simulations of Quench Test (17th October 2010), cell 14R2, beam 2 deflected in the vertical plane
- [14] A. Priebe, B. Dehning, M. Sapinski, M. Q. Tran, A. Verweij, "Investigations of quench limits of the LHC superconducting magnets", to be published in IEEE Transactions on Applied Superconductivity (IEEE-TAS)
- [15] A. Verweij, private communication
- [16] A. Lechner, Fluka simulations